ARTICLE IN PRESS
MARSYS-01531; No of Pages 22

Available online at www.sciencedirect.com
ScienceDirect
Journal of Marine Systems xx (2008) xxx – xxx
JOURNAL OF MARINE SYSTEMS
www.elsevier.com/locate/jmarsys

Air–sea fluxes and river discharges in the Black Sea with a focus on the Danube and Bosphorus

A. Birol Kara [a,*], Alan J. Wallcraft [a], Harley E. Hurlburt [a], E.V. Stanev [b,1]

[a] *Oceanography Division, Naval Research Laboratory, Stennis Space Center, MS, USA*
[b] *ICBM—Physical Oceanography, University of Oldenburg, Oldenburg, Germany*

Received 20 November 2006; received in revised form 9 June 2007; accepted 19 November 2007

Abstract

Climatological variations of thermal and haline buoyancy fluxes are investigated in the Black Sea. Analyses are performed to determine whether or not thermal buoyancy flux due to net heat flux (or haline buoyancy flux due to freshwater flux) dominates net buoyancy flux in the Black Sea. The effect of the two types of buoyancy flux are examined using a ≈3.2 km resolution HYbrid Coordinate Ocean Model (HYCOM). In the Black Sea, salinity is increased by Bosphorus inflow and decreased by precipitation and the inflow from six major rivers. Thus, the monthly mean discharge values from six major rivers are used as additions to the precipitation field in the model. River discharges are obtained from four climatologies: (1) River DIScharge (RivDIS), (2) Perry, (3) University Corporation for Atmospheric Research (UCAR) and (4) Naval Research Laboratory (NRL). Statistical evaluations of climatological river discharges from these products result in similar annual mean values. However, there are differences in the seasonal cycle. In the case of Danube, which has the largest annual river discharge contribution of ≈6365 $m^3 s^{-1}$, RMS differences for river discharge values over the seasonal cycle are within ≈2% among all products. The Black Sea HYCOM simulation uses climatological monthly mean atmospheric forcing (wind and thermal forcing) from European Centre for Medium-range Weather Forecast (ECMWF) Re-analyses. Buoyancy flux fields obtained from the HYCOM simulation demonstrate that thermal buoyancy flux dominates haline buoyancy flux in all months except March when the basin-averaged absolute ratio of former to the latter is 0.5 in the Black Sea. On the contrary, large buoyancy ratio values of ≫1 in other months explain the buoyancy is much more sensitive to variations in heating. It is also found that near the Bosphorus Strait in the Black Sea the strongly concentrated source of salty water typically penetrates into the deeper layers as a plume. Further analyses of mean buoyancy fluxes reveal nonexistence of deep convection in the Black Sea on climatological time scales.
© 2007 Elsevier B.V. All rights reserved.

Keywords: Black Sea; River discharge; Buoyancy flux; Air–sea flux; Climatology

1. Introduction

The ocean is driven by a combination of wind stress from the atmosphere, heat fluxes, freshwater flux resulting from evaporation, precipitation and runoff from rivers. Among these, the freshwater flux is of particular importance since the upper ocean undergoes a regular cycle of convection and re-stratification in response to the annual

* Corresponding author.
E-mail addresses: birol.kara@nrlssc.navy.mil (A.B. Kara), alan.wallcraft@nrlssc.navy.mil (A.J. Wallcraft), harley.hurlburt@nrlssc.navy.mil (H.E. Hurlburt), e.stanev@icbm.de (E.V. Stanev).
URL: http://www7320.nrlssc.navy.mi1 (A.B. Kara).
[1] Now at University of Ulster, School of Environmental Sciences, Cromore Road, Coleraine, Northern Ireland.

0924-7963/$ - see front matter © 2007 Elsevier B.V. All rights reserved.
doi:10.1016/j.jmarsys.2007.11.010

Please cite this article as: Kara, A.B., et al., Air–sea fluxes and river discharges in the Black Sea with a focus on the Danube and Bosphorus, J. Mar. Syst. (2008), doi:10.1016/j.jmarsys.2007.11.010

cycle of buoyancy fluxes at the sea surface (e.g., Webster, 1994; Marshall and Schott, 1999). Therefore, accurate determination of freshwater fluxes along with heat fluxes at the sea surface is of particular importance for many types of applications, including climate studies (e.g., Trenberth et al., 2001).

Freshwater discharge into the ocean basins has become increasingly important in global climate system (Miller et al., 1994; Wijffels, 2001; Dai and Trenberth, 2002). Proper estimates of continental freshwater discharge is particularly essential for small ocean basins, such the Black Sea where the river runoff substantially affects the salt balance, and freshwater fluxes maintain the stable stratification in the Black Sea (Oguz and Besiktepe, 1999; Stanev et al., 2003). In addition, there are many uncertainties in the existing heat flux climatologies constructed from local observations which are sparse in both time and space (e.g., Schrum et al., 2001).

The Black Sea, main focus of this paper, can be considered as an estuarine basin as there are rivers discharged in to the continental shelf (Fig. 1). In the northwestern shelf the river runoff is maintained by Danube, Dniepr and Dniestr. In addition to these rivers, Rioni, Sakarya, Kizilirmak and many other small ones discharge into the Black Sea. The narrow Bosphorus Strait plays an important role in determining the ventilation of the Black Sea (Ozsoy et al., 2001). Thus, a combination of heat and freshwater fluxes, river runoff and the Bosphorus outflow can have substantial impact on dynamical features of the Black Sea. A simple example is that the amount of river runoff in the continental shelf is closely tied to the Cold Intermediate Layer (CIL) formation (e.g., Oguz and Besiktepe, 1999). Buoyancy due to river runoff is also a contributing factor in maintaining the basin-wide cyclonic circulation (Oguz et al., 1995). This becomes very important especially in the northwestern shelf where the majority of freshwater discharge occurs. In particular, the Danube River can have substantial effect on the oceanographic features of the western Black Sea. This river has monthly mean river discharge values ranging from 4000 to 9000 $m^3 s^{-1}$ on climatological time scales (Vorosmarty et al., 1997, 1998), making it one of the word's largest rivers. By collecting its water over large part of Europe, this river integrates the atmospheric signal and creates an amplified forcing in the western Black Sea.

All of the factors mentioned above demonstrate the impact of river runoff effects in the Black Sea. Thus, accurate modeling of salinity is of particular importance in the region. Salinity gradients can influence both local circulation dynamics and other upper ocean features, such as the vertical stratification. The use of reliable river discharge values is therefore essential in numerical ocean modeling studies of the Black Sea. However, the problem is to decide which data source is most accurate and if any are sufficiently accurate. Traditionally, ocean general circulation model (OGCM) studies in the Black Sea made use of the river discharge values from two sources (Altman and Kumish, 1986; Staneva and Stanev, 1998). Both of these data sources reported river runoff values constructed from local measurements. Since then, there have been other readily available climatological river discharge values reported from a few global data sets. One aim of this paper

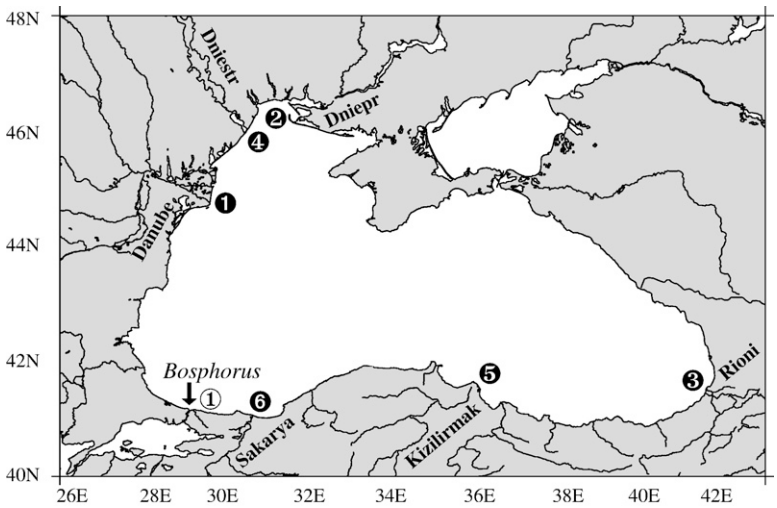

Fig. 1. Major rivers discharged into the Black Sea. The mouth of each river is shown with numbers from 1 to 6. The Bosphorus is the only source which is considered as negative precipitation (i.e., evaporation) source in the model simulation, which will be explained in Section 4, to close the evaporation–precipitation budget in the Black Sea. Kizilirmak, also known as Kizil, is the longest river in Turkey. It flows ≈ 1150 km from the central Turkish plateau, first to the southwest, then to the north and northeast into the Black Sea. The Sakarya River is the second largest river discharged into the Black Sea from Turkey.

Please cite this article as: Kara, A.B., et al., Air–sea fluxes and river discharges in the Black Sea with a focus on the Danube and Bosphorus, J. Mar. Syst. (2008), doi:10.1016/j.jmarsys.2007.11.010

is to discuss monthly and annual mean river flow values discharged into the Black Sea as constructed from these various climatologies. In addition, we would like to provide readily available river discharge values which can possibly be used for estuarine and OGCM studies in the Black Sea.

Assuming that heat and freshwater fluxes from operational models, such as European Centre for Medium-range Weather Forecast (ECMWF) data (Gibson et al., 1999), provide complete and reliable information at all temporal and spatial scales in comparison to climatologies formed from local observations in the Black Sea (e.g., Schrum et al., 2001; Kara et al., 2005a), they can be used for estimation of buoyancy fluxes. However, in a small region like the Black Sea, the grid resolution of ECMWF (1.125°×1.125°) is not appropriate to study small scale features due to river runoff. Even in the global ocean, there are large uncertainties arising from sparse observational coverage when studying the river runoff through freshwater fluxes and water mass formation (Wijffels et al., 1992; Doney et al., 1998). There are also problems with air–sea fluxes from model outputs (e.g., ECMWF), especially near the coastal regions. This is due mainly to land contamination of atmospheric variables within a grid box near the land–sea boundary (e.g., Kara et al., 2007). Therefore, it is appropriate to calculate sensible and latent heat fluxes based on the model SST using bulk formulations rather than obtaining them directly from ECMWF (e.g., Kara et al., 2005b,c). For these reasons, an OGCM can be useful for studying the impact of riverine and buoyancy fluxes, especially near coastal boundaries.

There are various studies, focusing on mixing processes at various regions of the Black Sea. For example, Oguz et al. (1990) studied internal hydraulics of the exchange processes in the Bosphorus Strait from/to the Black Sea based on a simple two-layer numerical model. Ozsoy et al. (2001) investigated mixing processes near the Bosphorus Strait and some coastal boundaries of the Black Sea. Stanev et al. (2003) examined the Cold Intermediate Water (CIW) formation with respect to buoyancy fluxes in the Black Sea, concluding that the region is dominated by dilution of surface waters by rivers while the seasonal variability is controlled by the air–sea fluxes. Korotaev et al. (2006) mentioned about possible effects of the buoyancy flux on the Black Sea circulation dynamics. One missing part in these earlier studies is the direct impact of river discharges on the buoyancy fluxes. Essentially, no specific consideration was given to river discharge values especially near the Bosphorus Strait and the Danube River.

To our knowledge, fine resolution spatial and temporal variations of surface buoyancy fluxes have not been examined in connection with river discharges in the Black Sea. To fill in this gap, the main focus in this paper is to examine freshwater fluxes with a particular attention to the river runoff based on up to date data sources and then use them in forcing a numerical ocean model. We will examine heat and freshwater fluxes along with thermal and haline buoyancy fluxes in the Black Sea using a fine resolution (≈3.2 km) hybrid coordinate OGCM, a model which includes mixed layer physics, river forcing treatment and atmospheric forcing.

In this study, we will analyze climatological mean river discharge values obtained from various sources, and investigate differences among them. Specifically, we put together the existing, but dispersed, data sets and assess them carefully. As presented in this paper, in detail, these data sets are also made available to the research community. A fine resolution OGCM is then forced with optimal monthly river flow values in addition to wind and thermal (e.g., solar radiation, near-surface air temperature) forcing. The model simulation is analyzed to study spatial and temporal variations of buoyancy fluxes in the Black Sea. Major purposes of examining the buoyancy fluxes in the Black Sea are to (1) determine the relative contributions of heat and freshwater fluxes to the surface buoyancy flux in the Black Sea, (2) identify the regions, where heat (freshwater) flux contribution to the surface buoyancy flux is significant.

This paper is organized as follows. Section 2 introduces the flow values for the rivers discharged into the Black Sea from various climatologies and explains how they were constructed. Section 3 compares monthly mean discharge values from these climatologies. Section 4 describes OGCM used in this paper, including a detailed examination of river flow treatment in the model and turbulence parameterizations. Section 5 presents buoyancy fluxes obtained from the model simulation over the Black Sea. Section 6 examines model-data comparisons. Section 7 gives conclusions of the paper.

2. River discharge climatologies for the Black Sea

There are six major rivers discharged into the Black Sea that are examined in this paper (Table 1), and the location of each river is shown in Fig. 1. Among these rivers, Danube has the largest upstream area of ≈807,000 km^2, followed by the Dniepr with an area of ≈463,000 km^2. Danube is the major European river to flow from west to east. It originates in Germany as two smaller rivers called Brigach Breg. These join in Donaueschingen, flowing south-east for a distance of about 2850 km, to the Black Sea in Romania where the Danube Delta is. The Dniepr River finds its source in

Please cite this article as: Kara, A.B., et al., Air–sea fluxes and river discharges in the Black Sea with a focus on the Danube and Bosphorus, J. Mar. Syst. (2008), doi:10.1016/j.jmarsys.2007.11.010

Table 1
A list of rivers discharged into the Black Sea

River	Station	Country	(Lat, Lon)	Area (km^2)
Danube	Power plant	Romania	(45.2°N, 29.7°E)	80,7000
Dniepr	Dniepr	Ukraine	(46.5°N, 32.3°E)	46,3000
Rioni	Sakochakidze	Georgia	(42.2°N, 41.6°E)	13,300
Dniestr	Bendery	Ukraine	(46.2°N, 30.1°E)	66,100
Sakarya	Botbasi	Turkey	(41.l°N, 30.7°E)	55,322
Kizilirmak	Inozu	Turkey	(41.7°N, 36.0°E)	75,121

The country represents where the river mouth is located. Latitude is the approximate latitude of the river mouth and longitude is the approximate longitude of the river mouth, both of which are based on the NRL river climatology as described in the text. Also given are station names and their upstream areas reported from the RivDIS climatology. Note that only those major rivers which are used in this study are provided.

north Russia and runs south eventually discharging into the Black Sea. Dniepr comes from Russia through Belarus and then Ukraine, and has a length of ≈2200 km. Dniestr rises in the Ukraine and flows toward the Black Sea. For a short distance it marks the border of Ukraine and Moldovia.

There are several monthly or annual river discharge climatologies constructed for the global ocean. These climatologies also include river flow values discharged into the Black Sea, one of the focuses of this paper. Before examining the monthly and annual mean river flow discharge values constructed from these sources, a brief explanation about each data source is provided here. As described below, there are mainly four climatologies (I through IV) from which river flow values discharged into the Black Sea are obtained.

(I) River DIScharge (RivDIS) climatology (Vorosmarty et al. 1997): This data set contains monthly discharge measurements for many stations located throughout the world. Table 2 gives climatological values for major rivers discharged into the Black Sea. Mean monthly discharge in $m^3 s^{-1}$ was derived by summing all available discharge measurements for a particular month and dividing by the number of measurements. Annual mean values were then calculated. The monthly mean values are shown in Fig. 2 for the rivers discharged into the Black Sea. The discharge values reported in this data set are measured through the use of a rating curve that relates local water level height to water flow. This rating curve is used to estimate discharge from the observed water level. The rating curves are periodically rechecked and re-calibrated through on-site measurement of discharge and river stage. Site attributes were checked for consistency through comparisons with the United Nations Educational, Scientific, and Cultural Organization (UNESCO) published series. Specifically, checks were made on the accuracy of the site names, locations, and contributing drainage areas.

(II) Perry climatology (Perry et al., 1996): The data set provides estimates of annual mean river discharges for 981 of the largest global rivers. It is meant to describe freshwater discharges to the oceans. Discharge values for as many rivers as possible were gathered from as many sources as possible. Often, this meant there were several values for a particular river. For each river, obvious errors and duplicated values were removed as explained in Perry et al. (1996). It was assumed that if two or more sources quote the same value, then they are probably referencing the same original source. For each river, the mean and standard deviation of the remaining values were calculated. Then values that were more than two standard deviations from the mean were eliminated as outlying values. The mean and standard deviation were then calculated a second time and those are the values used in this data set. The accuracy of the measurements is not given in the original sources. River gauging is generally thought to have an accuracy of 5–10% but the actual accuracy depends significantly on local conditions (Dingman 1994).

The annual mean flow values for the Black Sea rivers were compiled from different sources published in the literature (Table 3). In this list, the number of sources is the ones used to determine the arithmetic mean stream flow for a given river. However, this does not necessarily equal the overall number of sources found for that river since duplicate values and outliers are not used to determine the arithmetic mean stream flow. For example, there are 14 different sources for the Danube River but only 6 of them are used to calculate mean flow value (Table 4).

(III) University Corporation for Atmospheric Research (UCAR) climatology: Another global data base from UCAR contains real time monthly averaged river discharges. Geographic coverage of the joint set spans all major rivers and oceanographic basins around the global ocean, including the ones discharged into the Black Sea. This data set contains monthly river discharge rates for 4425 locations around the world. A problem with this data set is that the measurements are often too far from the mouth of the river to reliably represent the discharge into the ocean, limiting its usefulness in ocean modeling studies.

Please cite this article as: Kara, A.B., et al., Air–sea fluxes and river discharges in the Black Sea with a focus on the Danube and Bosphorus, J. Mar. Syst. (2008), doi:10.1016/j.jmarsys.2007.11.010

Table 2
Monthly climatological river discharge values ($m^3 s^{-1}$) from three different climatological data sets: (1) RivDIS, (2) UCAR and (3) NRL

	RivDlS monthly mean climatological river discharge values						
Month	Danube	Dniepr	Rioni	Dniestr	Sakarya	Kizilirmak	Total
Jan	5940.7	1369.0	302.4	207.1	267.9	212.9	8300.0
Feb	6219.5	1598.7	345.3	293.7	272.1	255.4	8984.7
Mar	7367.1	1672.9	429.8	550.6	295.2	328.4	10,644.0
Apr	8574.0	2477.6	652.9	615.1	269.9	308.2	12,897.7
May	8937.9	2893.1	610.1	460.1	183.0	231.2	13,315.4
Jun	8315.7	1616.6	533.6	502.8	146.7	157.0	11,272.4
Jul	7122.5	1057.6	426.9	475.5	122.8	118.2	9323.5
Aug	5519.1	941.9	325.4	348.8	110.8	123.8	7369.8
Sep	4703.8	841.5	240.2	288.4	112.0	147.4	6333.3
Oct	4446.5	979.8	293.7	247.3	123.6	167.6	6258.5
Nov	4996.0	1111.5	356.6	260.9	218.4	173.4	7116.8
Dec	5839.9	1240.9	385.1	250.2	191.8	202.6	8110.5
UCAR, monthly mean climatological river discharge values							
Jan	5881.4	1369.0	286.5	187.7	267.8	212.9	8205.3
Feb	6025.2	1602.1	350.9	231.8	272.3	256.1	8738.4
Mar	7255.5	1672.9	443.4	486.5	295.2	328.4	10,481.9
Apr	8607.9	2477.6	640.6	587.7	269.8	308.3	12,891.9
May	8898.9	2893.1	644.9	401.5	183.0	231.3	13,252.7
Jun	8185.5	1616.6	550.3	382.9	146.7	157.0	11,039.0
Jul	6917.8	1057.6	416.0	386.8	122.7	117.8	9018.7
Aug	5365.8	941.9	292.9	310.1	110.7	123.8	7145.2
Sep	4598.3	841.5	243.2	245.3	112.0	147.4	6187.7
Oct	4404.5	979.8	304.4	219.4	123.6	167.6	6199.3
Nov	4971.1	1111.5	321.3	231.1	218.3	173.4	7026.7
Dec	5850.9	1240.9	338.0	220.9	191.7	202.6	8045.0
NRL monthly mean climatological river discharge values							
Jan	5818.6	1505.0	303.3	180.2	301.9	212.9	8321.9
Feb	6091.6	1757.6	346.3	255.5	306.7	255.4	9013.1
Mar	7215.7	1839.1	431.1	479.0	332.7	328.4	10,626.0
Apr	8397.7	2723.8	654.8	535.1	304.2	308.2	12,923.8
May	8754.2	3180.6	611.9	400.3	206.3	231.2	13,384.5
Jun	8144.7	1777.2	535.2	437.4	165.3	157.0	11,216.8
Jul	6976.1	1162.7	428.2	413.7	138.4	118.2	9237.3
Aug	5405.6	1035.5	326.4	303.5	124.9	123.8	7319.7
Sep	4607.1	925.1	240.9	250.9	126.2	147.4	6297.6
Oct	4355.1	1077.2	294.6	215.2	139.3	167.6	6249.0
Nov	4893.3	1221.9	357.6	227.0	246.2	173.4	7119.4
Dec	5719.8	1364.2	386.2	217.7	216.2	202.6	8106.7

Total river discharges from all rivers are provided by month. The original global RivDIS data set is available online at http://daac.ornl.gov/rivdis/, and the global UCAR data set is available at http://dss.ucar.edu/datasets/ds552.1/. The NRL river climatology may be available upon request. Monthly mean discharge values for Dniepr are same for RivDIS and UCAR except February as both data sets use almost identical data sources during the same time period (1952–1984).

(IV) Naval Research Laboratory (NRL) climatology (Barron and Smedstad, 2002): The hypothesis used in constructing the global NRL river data set proposes that a database of monthly mean river discharges will be superior to a database of annual means in its ability to estimate real time discharge. The NRL river data set comes from Perry et al. (1996) which had one mean value for each river but the set was converted to monthly values to be used in ocean modeling studies.

A summary of the conversion to monthly mean values is provided here for the rivers discharged into the Black Sea. As a first step, monthly stream flow numbers were obtained from the electronically available RivDIS data set (http://www.daac.ornl.gov/daacpages/rivdis.html) to get

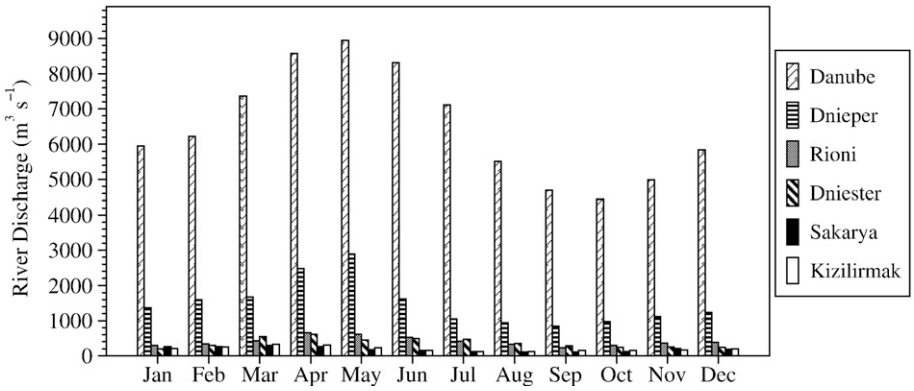

Fig. 2. Climatological monthly mean discharge values for six rivers discharged into the Black Sea as obtained from the RivDIS data set.

most global (non-USA) rivers. Once all the river inflow values were obtained, for most rivers the value that was largest (near the river outflow) and the most complete (longest time series of measurements and/or the least amount of missing values and/or the most recent values) were used. Finally, the annual mean value was scaled up the value reported in Perry et al. (1996) for each of the RivDIS rivers if the latter was larger, under the assumption that the smaller value resulted from stations further upriver. As a second step, monthly mean values were processed. The pertinent monthly mean data values from RivDIS were obtained for the Black Sea rivers, and each monthly average relation to the annual mean was figured out. All of these relative values were averaged if there was more than one.

For river stream flow or discharge data sets recording monthly means, which average to an annual transport smaller than that of the Perry data, there are three assumptions. (1) The (larger) Perry mean was determined using data downriver of the station used to derive the monthly means and is therefore a better estimate of the mean annual transport at the river mouth, (2) the variability described by the relative size of each river among the monthly means is a good proxy for the variability at the river mouth, and (3) thus, the monthly means at the river mouth would be scaled as (data set monthly mean) × (Perry annual mean)/(data set annual mean). The resulting climatological monthly mean values are shown in Table 2 for the rivers discharged into the Black Sea.

Table 3
Number of data sources in the Perry data set to be used in calculating the climatological annual mean river flow values discharged into the Black Sea

River	Number of sources		River discharge	
	Total	Used	(m^3 s^{-1})	(km^3 s^{-1})
Danube	14	7	6365.0	203.7
Dniepr	10	6	1630.8	52.2
Rioni	3	3	409.7	13.1
Dniestr	4	4	326.3	10.4
Sakarya	3	3	217.3	7.0
Kizilirmak	2	2	180.5	5.8

Note that duplicated sources were eliminated from total sources for annual mean discharge calculations.

3. Black Sea river climatology comparisons

The river discharge climatology is formed for each river over various time periods based on the availability of the data (Table 5). The Perry data set was constructed using annual mean at individual years so the total number of years represents total of these individual years. On the contrary, we constructed the climatological discharge values from RivDIS and UCAR using monthly mean discharge values for each consecutive year during the time period. Annual mean discharge values shown in Fig. 3 clearly reveal that Danube has the largest river flow contribution (≈ 70%).

A scatter plot of river discharge values among different climatologies clearly demonstrates good agreement, while there exist some deviations for Dniestr and Sakarya (Fig. 4). Some differences between NRL and other climatologies arise because the river discharge from NRL is scaled to the value proportional to that from the Perry climatology. Thus, the monthly mean value is a linear operation on the RivDIS numbers and is not very different from them. Specifically, a version of the RivDIS database was used as one of several inputs to the NRL database. In the case of the rivers discharged into the Black Sea, most RivDIS data were the result of measurement ending as far back as 1984. Annual mean data from (Perry et al., 1996) was more recent and was assumed to be more correct and more near to the river mouth. Thus, the monthly means for

Table 4
List of references used in the Perry data to obtain annual mean flow values for each river discharged into the Black Sea

Discharge (m^3 s^{-1})	Reference	Discharge (m^3 s^{-1})	Reference
Danube		Dniepr	
6550	Milliman and Meade (1983)	1700	Kammerer (1989)
6500	Kammerer (1989)	1700	Dynesius and Nilsson (1994)
6500	UNESCO (1985)	1670	van der Leeden et al. (1990)
6450	Showers (1979)	1670	Leopold (1962)
6450	Dynesius and Nilsson (1994)	1660	Kempe et al. (1991)
6450	Czaya (1981)	1660	Degens et al. (1991)
6450	Kempe et al. (1991)	1650	Meybeck (1988)
6430	Meybeck (1988)	1620	Showers (1979)
6250	Kempe et al. (1991)	1485	UNESCO (1985)
6250	Degens et al. (1991)	1160	Czaya (1981)
6250	van der Leeden (1975)	Rioni	
6200	Szestay (1982)	409	UNESCO (1985)
6175	van der Leeden et al. (1990)	420	Dynesius and Nilsson (1994)
6175	Leopold (1962)	400	van der Leeden (1975)
Sakarya		Dniestr	
202	van der Leeden (1975)	377	UNESCO (1985)
257	Showers (1979)	311	Kempe et al. (1991)
193	UNESCO (1985)	310	Showers (1979)
Kizilirmak		307	van der Leeden (1975)
202	UNESCO (1985)		
159	van der Leeden (1975)		

Discharge values in this data set for as many rivers as possible were gathered from as many sources as possible.

the rivers in RivDIS were scaled to calculate monthly means proportional to the annual mean by multiplying the Perry annual mean and then dividing by the RivDIS annual mean.

Statistical analysis is performed to further examine errors in monthly mean discharge values between the climatological data set pairs. Following Murphy (1988), the statistical relationships used here between the monthly mean river discharge values from RivDIS (X) and NRL (Y) can be expressed as follows:

$$\mathrm{ME} = \overline{Y} - \overline{X}, \tag{1}$$

$$\mathrm{RMS} = \left[\frac{1}{n}\sum_{i=1}^{n}(Y_i - X_i)^2\right]^{1/2}, \tag{2}$$

$$\mathrm{NRMS}^2 = \frac{1}{n}\sum_{i=1}^{n}\left[\frac{(Y_i - X_i)}{X_i}\right]^2, \tag{3}$$

$$R = \frac{1}{n}\sum_{i=1}^{n}(X_i - \overline{X})(Y_i - \overline{Y})/(\sigma_X \sigma_Y), \tag{4}$$

$$\mathrm{SS} = R^2 - \underbrace{[R - (\sigma_Y/\sigma_X)]^2}_{B_{\mathrm{cond}}} - \underbrace{[(\overline{Y} - \overline{X})/\sigma_X]^2}_{B_{\mathrm{uncond}}}, \tag{5}$$

where $n = 12$ (months), ME is the mean error, RMS is the root-mean-square difference, NRMS is the normalized RMS, R is the correlation coefficient, SS is the skill score, and $\overline{X}(\overline{Y})$ and σ_X (σ_Y) are the mean and standard deviations of the RivDIS (NRL) discharge values, respectively. Because the NRL climatology is based on an estimate, it is always considered as a dependent variable (i.e., Y) in comparisons. Note that RivDIS is considered as a reference data set because it is independent of the Perry data and assumed to be more accurate than UCAR for ocean modeling studies as the UCAR data set does not report discharge values at the river mouth. When comparing the UCAR climatology with the NRL

Table 5
Time periods over which climatological river discharges were constructed

River	Perry		RivDIS		UCAR	
	Climatology	Year	Climatology	Year	Climatology	Year
Danube	1921–1994	14	1921–1984	64	1921–2000	80
Dniepr	1962–1994	10	1952–1984	33	1952–1984	33
Rioni	1975–1994	3	1965–1984	20	1928–1984	57
Dniestr	1975–1991	4	1965–1984	20	1881–1985	76
Sakarya	1975–1991	3	1976–1983	8	1976–1983	8
Kizilirmak	1975–1991	2	1976–1983	8	1976–1983	8

Total number of years for the climatology is also included. The NRL data set was created using mainly the Perry data set so the time period over which the NRL climatology was constructed is the same as the Perry data set.

Please cite this article as: Kara, A.B., et al., Air–sea fluxes and river discharges in the Black Sea with a focus on the Danube and Bosphorus, J. Mar. Syst. (2008), doi:10.1016/j.jmarsys.2007.11.010

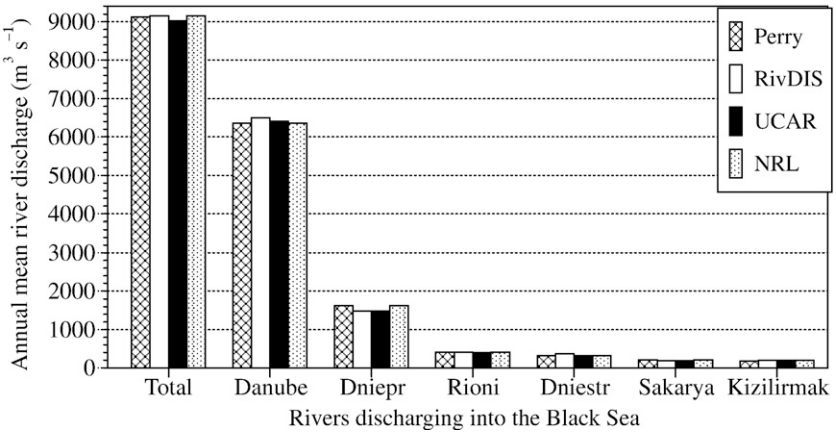

Fig. 3. Annual mean flow values from various climatological data sources for the major rivers discharged into the Black Sea. The annual mean discharge value for each river is calculated using climatological monthly mean discharge values. Also provided is the total annual mean flow discharge from all rivers. Danube and Dniepr provides most of river discharges to the Black Sea, 69.72% and 17.86% of the total, respectively. Contributions to the total river discharge from other rivers are very small with values of 4.49%, 3.57%, 2.38% and 1.98% for Rioni, Dniestr, Sakarya and Kizilirmak, respectively. The percentage values were calculated using annual mean values from the Perry climatology as shown in the figure.

climatology, the former is considered as the reference data set (i.e., X) because it is an independently created data set.

The non-dimensional SS which includes conditional and unconditional biases in Eq. (5) is also used because we need to examine more than the shape of the seasonal cycle using R. The SS measures the accuracy[2] of NRL discharge values relative to RivDIS. The conditional bias (B_{cond}) is the bias in standard deviation of the NRL discharges, while the unconditional bias (B_{uncond}) reflects the mismatch between the mean NRL and RivDIS. Skill score is 1.0 for perfect NRL discharge values. The NRMS is also a measure of the relative distance between the estimate and reference. The scaling factors have different meanings for SS and NRMS. Both non-dimensional metrics are used to obtain further information about differences in the river discharge values.

There is clearly a good agreement between RivDIS and UCAR (see also Fig. 4), with small ME and RMS values for each river (Table 6). Almost all of the variance (100%) in the RivDIS discharge values is reproduced by the NRL and UCAR as evident the square of all R values. All R values are >0.8. For the 12 monthly river discharge values the R value must be at least ± 0.53 for it to be statistically different from a correlation coefficient of zero based on the student's t test at the 95% confidence interval (Neter et al., 1988). The SS values are very high, being very close to 1. This indicates almost a perfect agreement among all data sets although the NRMS values for UCAR discharge values vary from 0.05% to 10% of the RivDIS discharge values. The largest error is seen for Dniestr. In the case of RivDIS versus NRL and UCAR versus NRL pairs, RMS and ME values are slightly larger than those for the RivDIS versus UCAR pair. In the case of Dniestr the NRMS value is largest, indicating discrepancies over the annual cycle in all data set. A remarkable agreement is evident at Danube, which has the largest discharge values in the region. The river discharge estimate for Danube differs only with $\approx 2\%$ among all climatologies. In summary, as evident from positive and large SS values, the reasonable agreement in discharge values for all rivers is quite remarkable given the uncertainties and measurement errors in the climatological data sets.

It is emphasized that in the cases of rivers discharged into the Black Sea, the RivDIS database was used to determine NRL river database. Most RivDIS data resulted from measurements ending as far back as 1984 as indicated previously (Table 5). In most cases the annual mean from the Perry climatology was larger, corresponding to a closer location to a river mouth. The exceptions to this were the Danube River, where the mean from the Perry climatology was only slightly smaller, $\approx 2\%$, and the Dniestr River, where the mean was $\approx 13\%$ smaller.

4. Ocean model description

The Black Sea simulation is performed using a fine resolution (≈ 3.2 km) HYbrid Coordinate Ocean Model (HYCOM) to examine buoyancy fluxes. Details of HYCOM equations are given in Bleck (2002). The vertical coordinate evaluation for HYCOM is discussed in

[2] Note here that accuracy refers to the match between RivDIS and NRL discharge values, and skill refers to the NRL discharge accuracy relative to the RivDIS climatology.

Please cite this article as: Kara, A.B., et al., Air–sea fluxes and river discharges in the Black Sea with a focus on the Danube and Bosphorus, J. Mar. Syst. (2008), doi:10.1016/j.jmarsys.2007.11.010

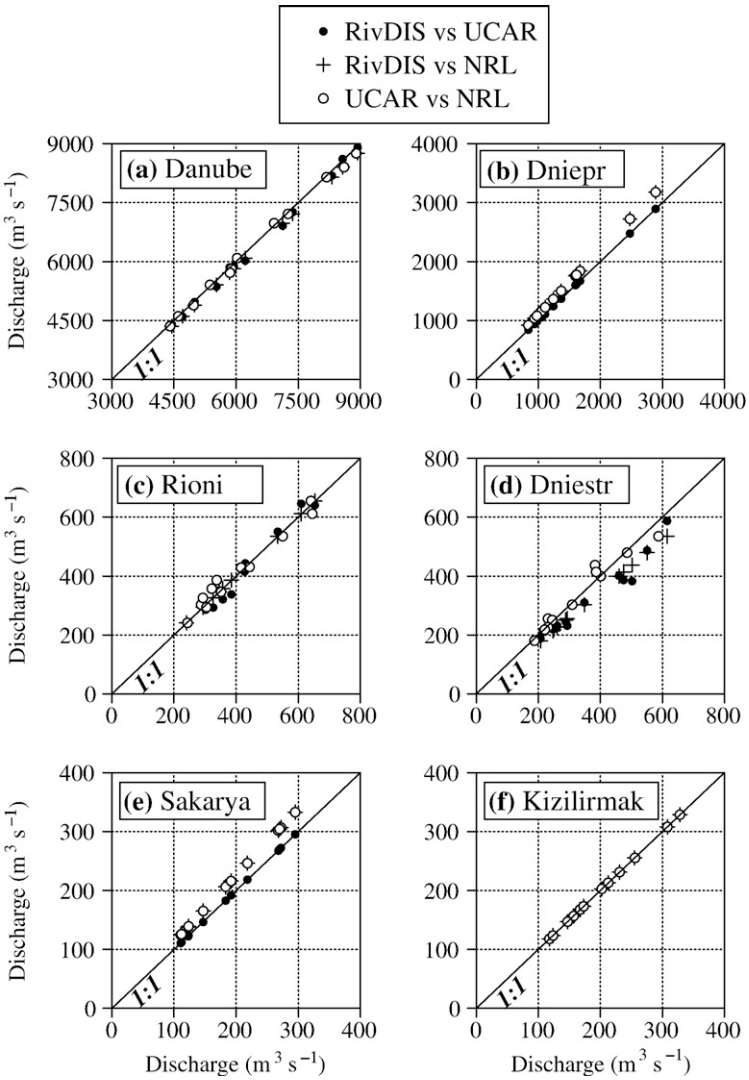

Fig. 4. Scatter diagram of climatological monthly mean flow values among different climatological data sets. Comparisons are shown at each individual river discharged into the Black Sea.

Chassignet et al. (2003); the vertical mixing algorithms are provided in Halliwell (2004); the Black Sea model set up is given in Kara et al. (2005b).

The model combines the advantages of the isopycnal, σ and partial-cell z-level coordinates within a single framework in optimally simulating coastal and open-ocean circulation features in the Black Sea. In particular, the model uses hybrid vertical coordinate grid generator and the layered continuity equation to make a dynamically smooth transition from isopycnal coordinates in the stratified ocean to a terrain-following coordinate in shallow coastal regions, and to z-level coordinates in the mixed layer and/or unstratified seas. We made several modifications to the original hybrid generator routine. In summary, the original approach can lead to excessive diffusion when remapping layers that are far from isopycnal. The modified HYCOM remapper used here allows the profile to vary linearly across a layer when the layer is not close to being isopycnal, thus significantly reducing numerical diffusion.

4.1. Mixed layer parameterizations

The assured presence of uniformly spaced coordinate layers in the upper ocean allows the formulation of turbulent near-surface mixing. The K-Profile-Parameterization (KPP) is the first non-slab mixed layer model

Table 6
Statistical comparisons of the river discharge values between various climatological data pairs for each river discharged into the Black Sea

River	RMS ($m^3 s^{-1}$)	ME ($m^3 s^{-1}$)	R	SS	NMRS	NMRS (%)
RivDIS versus UCAR, discharge values						
Danube	112.7	−85.0	1.00	0.99	1.8e−2	1.8
Dniepr	1.0	0.3	1.00	1.00	6.le−4	0.1
Rioni	23.9	−5.8	0.99	0.96	6.2e−2	6.2
Dniestr	58.2	−50.7	0.98	0.81	0.le−0	10.0
Sakarya	0.1	0.0	1.00	1.00	4.8e−4	0.1
Kizilirmak	0.2	0.0	1.00	1.00	1.3e−3	0.1
RivDIS versus NRL discharge values						
Danube	137.0	−133.6	1.00	0.99	2.le−2	2.1
Dniepr	159.2	147.4	1.00	0.93	9.9e−2	9.9
Rioni	1.3	1.2	1.00	1.00	3.0e−3	0.3
Dniestr	51.7	−48.8	1.00	0.85	1.3e−1	13.0
Sakarya	26.0	24.5	1.00	0.85	1.3e−1	13.0
Kizilirmak	0.0	0.0	1.00	1.00	0.0e−0	0.00
UCAR versus NRL discharge values						
Danube	94.6	48.6	1.00	0.99	1.3e−2	1.3
Dniepr	158.0	−147.1	1.00	0.94	9.9e−2	9.9
Rioni	24.1	−7.0	0.99	0.96	6.9e−2	6.9
Dniestr	24.6	−2.0	0.98	0.95	6.3e−2	6.3
Sakarya	26.0	−24.5	1.00	0.88	1.3e−1	13.0
Kizilirmak	0.2	0.0	1.00	1.00	1.3e−3	0.1

A detailed description of the statistical parameters is given in the text.

(Large et al., 1997) included in HYCOM. In the ocean interior, the contribution of background internal wave breaking, shear instability mixing, and double diffusion (both salt fingering and diffusive instability) are formulated. In the surface boundary layer, the influences of wind-driven mixing, surface buoyancy fluxes, and convective instability are parameterized. The KPP algorithm also accounts for the influence of non-local mixing of temperature and salinity, which permits the development of counter gradient fluxes.

The major focus of this paper is to examine surface buoyancy fluxes over the Black Sea. Thus, we only present parameterizations which are related to the buoyancy fluxes. In the model, buoyancy flux (B_f) and buoyancy (B) are expressed as follows:

$$B_f = -\frac{g\alpha(T_s, S_s)Q_a}{\rho_o C_w} + g\beta(T_s, S_s)(E - P)S_s, \quad (6)$$

$$B = \alpha(T_s, S_s)T - \beta(T_s, S_s)S, \quad (7)$$

$$\alpha(T_s, S_s) = \frac{\partial\rho/\partial T}{\rho_o}, \quad (8)$$

$$\beta(T_s, S_s) = \frac{\partial\rho/\partial S}{\rho_o}, \quad (9)$$

where g is the gravitational acceleration (9.81 m s^{-1}), $\alpha(T_s, S_s)$ is the thermal expansion coefficient (°C^{-1}), P (T_s, S_s) is salt expansion coefficient (psu^{-1}), T_s, is the sea surface temperature (°C), S_s, is the sea surface salinity (psu), ρ is the density (kg m^{-3}), p, is the reference density (1000 kg m^{-3}), Q_a is the net heat flux at the sea surface (W m^{-2}), C_w is the ratio of interior local buoyancy frequency to that at entrainment depth (a constant between 1 and 2). In (6) E is the evaporation due to latent heat (m s^{-1}), P is the precipitation due to rain (or snow) and river discharges (m s^{-1}), and they are discussed in Section 4.3, in detail. Expansion coefficients for temperature and salinity are calculated from the equation of state as explained in Brydon et al. (1999).

It is noted that B_f in (6) includes contributions from both heat flux and freshwater flux at the sea surface. Positive (negative) buoyancy flux indicates a buoyancy loss (gain). Surface density increases (i.e., water column is destabilized) if $B_f > 0$, and surface density decreases (i.e., water column is stabilized) if $B_f < 0$. Net heat and freshwater fluxes at the sea surface are defined as positive quantities into the ocean. In addition, B in (7) is a function of the relative density of an ocean parcel compared with its neighbor.

4.2. Black Sea model

The Black Sea model has a 1/25° × 1/25° cos(lat), (longitude × latitude) square mercator grid. Average grid

resolution is 3.2 km, ranging from a minimum of 3.05 km to a maximum of 3.37 km in the Black Sea. The model includes realistic bottom topography constructed from the 1 min data obtained from the U.S. Naval Oceanographic Office (NAVOCEANO). The climatologically-forced Black Sea HYCOM simulation presented in this paper was performed with no assimilation of any oceanic data including SST. This is done to examine first order effects of atmospheric forcing on the model simulation. The model is initialized using the temperature and salinity profiles from the Modular Ocean Data Assimilation System (MODAS), as described in Kara et al. (2005b). The climatology is used only for initialization and surface salinity relaxation. The model simulation includes no relaxation to any data except a relaxation to monthly mean sea surface salinity from MODAS. The model simulation was run for eight years using the 6-hourly climatological forcing as will be described below. It takes about four model years for a simulation to reach equilibrium. For evaluation of the model results, monthly mean model fields were formed from daily outputs using the last 4 model years (years 5 through 8). The reader is referred to Kara et al. (2005b,c) for further details of the model.

HYCOM reads in the following time-varying atmospheric forcing fields: wind stress, wind speed and thermal forcing (air temperature, air mixing ratio, shortwave radiation, and net solar radiation). In this paper, the HYCOM simulation uses monthly mean wind/thermal forcing based on ECMWF 15 year Re-Analysis (ERA-15) formed over 1979–1993. The ERA product has a grid resolution of $1.125° \times 1.125°$. Previous simulations revealed that the use of the ERA forcing results in reliable results in predicting upper ocean variables (Kara et al., 2005c). The model run is performed using climatological monthly mean forcing fields interpolated to daily values. A high frequency component (6 hourly) is added to the climatological wind forcing, whose details and applications are given in Kara et al. (2005a).

The net heat flux absorbed from the sea surface down to depth z ($Q(z)$) is given as follows:

$$Q(z) = Q(0) + (Q_{\mathrm{sol}}(0) - Q_{\mathrm{sol}}(z)), \tag{10}$$

$$Q(0) = Q_{\mathrm{LW}} + Q_{\mathrm{L}} + Q_{\mathrm{S}}, \tag{11}$$

$$Q_{\mathrm{sol}}(z)/Q_{\mathrm{sol}}(0) = (1-\gamma)\exp(-z/0.5) + \gamma\exp(-zk_{\mathrm{PAR}}), \tag{12}$$

$$\gamma = \max(0.27, 0.695 - 5.7k_{\mathrm{PAR}}) \tag{13}$$

where $Q(0)$ is net heat flux absorbed at the sea surface, $Q_{\mathrm{so1}}(0)$ is total shortwave radiation at the sea surface, $Q_{\mathrm{sol}}(z)$ is remaining (unabsorbed) shortwave radiation at depth z, Q_{Lw} is the downward net longwave radiation, Q_{L} is the downward latent heat flux and Q_{s} is the sensible heat flux. The HYCOM's "surface" heat flux is not $Q(0)$, but rather the near-surface flux absorbed in layer 1 (Q (3 m) when the top model layer is 3 m thick). Thus, $Q(0)$ in Eq. (11) does not include $Q_{\mathrm{so1}}(0)$. None of $Q_{\mathrm{so1}}(0)$ is absorbed at the surface although $(1-\gamma)$% is absorbed very near the surface. The model reads in spatially and temporally varying satellite-based monthly mean attenuation of Photosynthetically Available Radiation (k_{PAR}) fields to include effects of turbidity in the shortwave radiation penetration. In Eq. (12), the red penetration scale is 2 m, and the blue penetration scale is $1/k_{\mathrm{PAR}}$.

Net solar radiation (net shortwave radiation plus net longwave radiation) is so dependent on cloudiness that this is taken directly from ECMWF, except for a modification to longwave radiation based on model SST (Kara et al., 2005c). Both Q_{L} and Q_{s} in Eq. (11) are calculated using model SST and the bulk formulations that use stability-dependent exchange coefficients at each model time step (Kara et al., 2005e). Basing Q_{L} and Q_{s} on the model SST automatically provides a physically realistic tendency towards the correct model SST.

4.3. River runoff in the Black Sea model

HYCOM treats rivers as a runoff addition to the surface precipitation field. The flow is first applied to a single ocean grid point and smoothed over surrounding ocean grid points, yielding a contribution to precipitation in m s^{-1}. In the Black Sea model, there are a total of six major rivers (Section 2).

In general, the Black Sea has a positive freshwater flux resulting from excess precipitation and river runoff over evaporation. This positive excess can be considered to be equal to the transport in the Bosphorus Strait (Unluata et al., 1990). The reason is that while it is not thoroughly confirmed, the Bosphorus has generally a flow system, such that less saline and lighter water exists from the Black Sea via Bosphorus at the surface, while the saltier and denser Mediterranean water flow into the Black Sea as underflow. Thus, the transport through the strait compensate for the dilution at the sea surface and could be considered to contribute to the evaporation. Because the simulations presented in this paper are carried out in a closed basin configuration, the excess of precipitation and river runoff over evaporation, if exists, in the model must be removed by the strait outflow, leading to a zero salt balance in the Black Sea.

Please cite this article as: Kara, A.B., et al., Air–sea fluxes and river discharges in the Black Sea with a focus on the Danube and Bosphorus, J. Mar. Syst. (2008), doi:10.1016/j.jmarsys.2007.11.010

We express the net water balance (P_{net}) in the Black Sea as follows:

$$P_{net} = E + P + P_{River} + P_{Bosp.}, \tag{14}$$

where E is evaporation, P is precipitation due to rain or snow, P_{River} is precipitation due to rivers, and $P_{Bosp.}$ is negative precipitation due to the transport from the Bosphorus Strait. HYCOM uses P from the ERA-15 as an atmospheric forcing, and P_{River} is from the RivDIS which is comparable to NRL and UCAR climatologies (see Section 3).

As evident from the net water balance given in Eq. (14), the Black Sea model treats rivers as a "runoff" addition to the surface precipitation field, and the Bosphorus Strait as a negative river precipitation (i.e., a river evaporation) to close freshwater flux balance. The basin-averaged values of the components of P_{net} are provided in Table 7. Although E is calculated in the model (i.e., it is not a prescribed forcing) using simulated latent heat flux at each time step, its values are provided to explain freshwater balance. Basin-averaged annual mean E (P) values are −270.2 (221.2) km^3 year^{-1} for ECMWF.

The P_{River} values are calculated using monthly mean discharge values from RivDIS (see Table 2 for individual monthly discharge values). The monthly mean Bosphorus outflow values are taken from Staneva and Stanev (1998). The monthly mean P_{River}, and $P_{Bosp.}$ values given in the table are calculated using the surface area of the Black Sea ($\approx 4.05\times10^5$ km^2) to be consistent with the basin-averaged E and P values. The annual mean bias value of 0.5 km^3 year^{-1} is used to remove the excess of precipitation and river runoff over evaporation in the model (Table 7). This bias mostly accounts for runoff values from many small rivers which were not used in the model simulations.

Table 7
Basin averaged monthly and annual mean evaporation (E), precipitation (P) values for the Black Sea

	ECMWF (km^3 year^{-1})		River flow discharges (km^3 year^{-1})			($E+P+P_{total}$) (km^3 year^{-1})
	E	P	P_{River}	$P_{Bosp.}$	P_{total}	
Jan	−265.5	267.2	260.3	−215.5	44.8	46.5
Feb	−241.3	220.3	281.7	−207.0	74.7	53.7
Mar	−144.6	185.3	333.9	−190.1	143.8	184.5
Apr	−91.7	238.4	404.1	−221.8	182.3	329.0
May	−108.0	231.4	417.6	−175.3	242.3	365.7
Jun	−195.2	233.0	353.6	−185.9	167.7	205.5
Jul	−315.8	222.6	292.5	−221.8	70.7	−22.5
Aug	−406.4	165.3	231.2	−234.5	−3.3	−244.4
Sep	−489.8	196.2	198.7	−249.3	−50.6	−344.2
Oct	−426.9	216.5	196.2	−245.1	−48.9	−259.3
Nov	−385.9	308.0	223.0	−236.6	−13.6	−91.5
Dec	−281.4	269.7	254.2	−217.6	36.6	24.9
Ann	−270.2	221.2	287.3	−216.7	70.5	0.5

River flow discharges include contributions from the total of 6 rivers (P_{River}) and from Bosphorus outflow ($P_{Bosp.}$).Note that P_{total} is the sum of river discharges used in HYCOM (i.e., $P_{River}+P_{Bosp.}$).The values in km^3 year^{-1} is obtained by multiplying flow values in km year^{-1} with the surface area of the Black Sea as used in the model domain ($\approx 4.05\times10^5$ km^2). The unit conversions used are 1 m s^{-1}=$10^{-3}\times30\times24\times60\times60$ mm month^{-1}, and 1 m s^{-1}=$\times365\times24\times60\times60$ km year^{-1}. In the table the "+" sign indicates a gain to ocean, and "–" sign indicates a loss from ocean.

5. Buoyancy fluxes over the Black Sea

In order to investigate the oceanic response to the atmospheric forcing (heat and freshwater fluxes) the buoyancy fluxes obtained from the model simulation are presented for the Black Sea. The buoyancy flux expression given in Eq. (7) consists of two terms: (1) thermal buoyancy flux, and (2) haline buoyancy flux. The thermal buoyancy flux is the buoyancy due to the net heat flux at the sea surface, and the haline buoyancy flux is the one due to the net freshwater flux at the sea surface. Thus, the total buoyancy is rewritten by rearranging (7) as follows:

$$B_f = \underbrace{-\frac{g}{\rho_o}\left[\frac{\alpha(T_s,S_s)Q_a}{C_w}\right]}_{\text{Thermal buoyancy flux}} + \underbrace{\frac{g}{\rho_o}[\rho_o\beta(T_s,S_s)(E-P)S_s]}_{\text{Haline buoyancy flux}}. \tag{15}$$

Hereinafter, P is used simplicity to represent the total precipitation (i.e., the sum of P_{River}, and $P_{Bosp.}$). The monthly means of total buoyancy fluxes along with its components (thermal and haline buoyancy fluxes) are presented (Fig. 5). The monthly fields were constructed from the daily model outputs. As mentioned earlier, negative buoyancy flux indicates a buoyancy gain while positive buoyancy flux indicates a buoyancy loss. The basin-averaged monthly mean values clearly reveal no strong seasonal cycle in buoyancy fluxes over the Black Sea (Fig. 6). A buoyancy gain is evident in most of the Black Sea from March through September on the climatological time scales (Fig. 5a). Such a gain simply reveals that the upper ocean is effectively stabilized during this time period. This buoyancy gain is associated with high solar heating in summer. In particular, relatively large (on the order of -10^{-7} m^2 s^{-3}) total buoyancy fluxes are particularly noted from May to July. On the other hand, there is a substantial buoyancy loss, especially in the northwestern shelf with values $>5\times10^{-8}$ m^2 s^{-3} in January and even 10^{-7} m^2 s^{-3} in November.

Please cite this article as: Kara, A.B., et al., Air–sea fluxes and river discharges in the Black Sea with a focus on the Danube and Bosphorus, J. Mar. Syst. (2008), doi:10.1016/j.jmarsys.2007.11.010

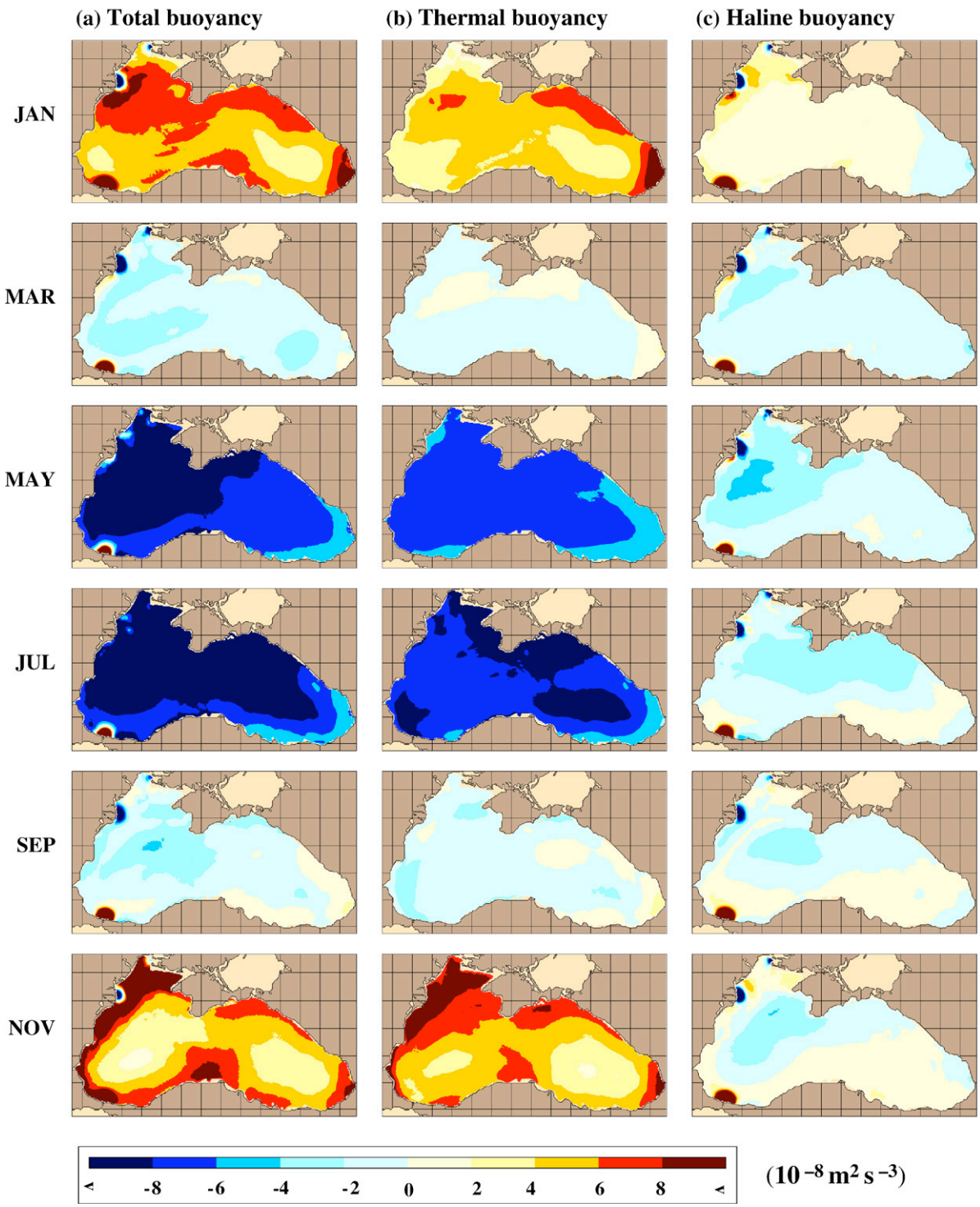

Fig. 5. Spatial and temporal variations of buoyancy fluxes obtained from the ≈3.2 km resolution HYCOM forced with ECMWF wind/thermal fluxes in the Black Sea. From top to bottom: (a) total buoyancy flux, (b) thermal buoyancy flux, and (c) saline buoyancy flux. All values are in 10^{-8} m^2 s^{-3}, and the results are shown for every other month. The surface buoyancy forcing is sum of the thermal buoyancy flux and saline buoyancy flux. In the color bar < denotes smaller (larger) values than seen at the edges.

Please cite this article as: Kara, A.B., et al., Air–sea fluxes and river discharges in the Black Sea with a focus on the Danube and Bosphorus, J. Mar. Syst. (2008), doi:10.1016/j.jmarsys.2007.11.010

ARTICLE IN PRESS

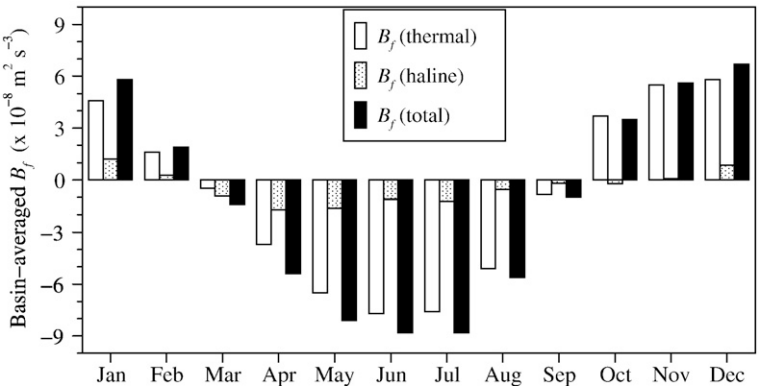

Fig. 6. The basin-averaged monthly mean total buoyancy flux and its components. They are based on the fields given in Fig. 5.

Consistent with the total buoyancy flux, both the thermal and haline buoyancy fluxes tend to stabilize the water from March through September over the most of the Black Sea (Fig. 5b,c). The basin-averaged buoyancy fluxes further confirm the buoyancy gain in these months (Fig. 6). On the contrary, both thermal and haline buoyancy fluxes result in destabilization in January, February, November and December. While annual mean net heat flux is zero over the Black Sea, there is no reason to expect basin-averaged zero mean annual buoyancy flux, which might result from slight changes in mean salinity in very long time scales.

Using Eq. (15), the absolute value of the buoyancy ratio ($|R|$) of the thermal and haline buoyancy flux components is given by

$$|R| = \left| \frac{\alpha(T_s, S_s) Q_a}{\rho_o C_w \beta(T_s, S_s)(E - P) S_s} \right|, \tag{16}$$

where the ratio, $|R|$, indicates the relative impact on upper ocean buoyancy of heating and salinity effects. From (16), $|R| \approx 1$(i.e., the absolute value of the ratio which is on order of unity) explains that the buoyancy appears to be equally affected by heating and salinity effects. In other words, heat and freshwater fluxes are of the same magnitude. In a similar analogy, heat flux dominates freshwater flux when $|R| \gg 1$ (i.e., the buoyancy is due mostly to net heat flux at the sea surface), and freshwater flux dominates heat fluxes when $|R| \ll 1$ (i.e., the buoyancy is due mostly to net freshwater flux at the sea surface).

The spatially and temporally varying $|R|$ values in Fig. 7a calculated using thermal and haline buoyancy fluxvalues (Fig. 5b,c) demonstrate that net heat flux dominates freshwater flux on the Black Sea on the climatological time scales. Also shown are net heat and freshwater fluxes at the sea surface (Fig. 7b,c), which are used for calculating thermal and haline buoyancy flux values. As evident from the figure, there are large gradients of P–E flux, especially near Danube. This is because river discharge values in HYCOM are considered as additions to the precipitation fields. The same is also true for the Bosphorus which is treated as a negative precipitation source in the model.

The only month when thermal buoyancy flux destabilizes the upper ocean but haline buoyancy flux stabilizes the upper ocean is October (Fig. 6). Because the thermal buoyancy flux is a factor of 16.8 larger than the haline buoyancy flux in October (Fig. 8), the upper ocean destabilizes and turbulence mixing is expected during the predawn rainfall in the Black Sea. The net surface buoyancy flux also destabilizes the water column in January, February, November and December, which is an indication of the generation of strong turbulent mixing. Consequently, precipitation tends to be balanced by mixing and does not produce anomalous surface freshening. The freshwater fluxes show great similarities with large values during this time period (Fig. 7b,c). Thus, turbulent mixing has a pronounced monthly variability in the Black Sea. Such a variability in the turbulent mixing results in dissipation of predawn rainfall that mixed downward through the mixed layer. In HYCOM, the stability of stratification is ensured by the fact treating Bosphorus as a negative precipitation source is very local. This treatment does not produce significant mixing over large areas away from the Bosphorus Strait (see Section 6).

In addition to the thermal buoyancy flux, an examination of the freshwater flux clearly reveals that precipitation is the likely reason for the existence of shallow mixed layer formation due to reduced turbulent mixing in the Black Sea during spring and summer. Note that very shallow mixed layer depths were noted in Kara et al. (2005d). For example, the net freshwater flux is

Please cite this article as: Kara, A.B., et al., Air–sea fluxes and river discharges in the Black Sea with a focus on the Danube and Bosphorus, J. Mar. Syst. (2008), doi:10.1016/j.jmarsys.2007.11.010

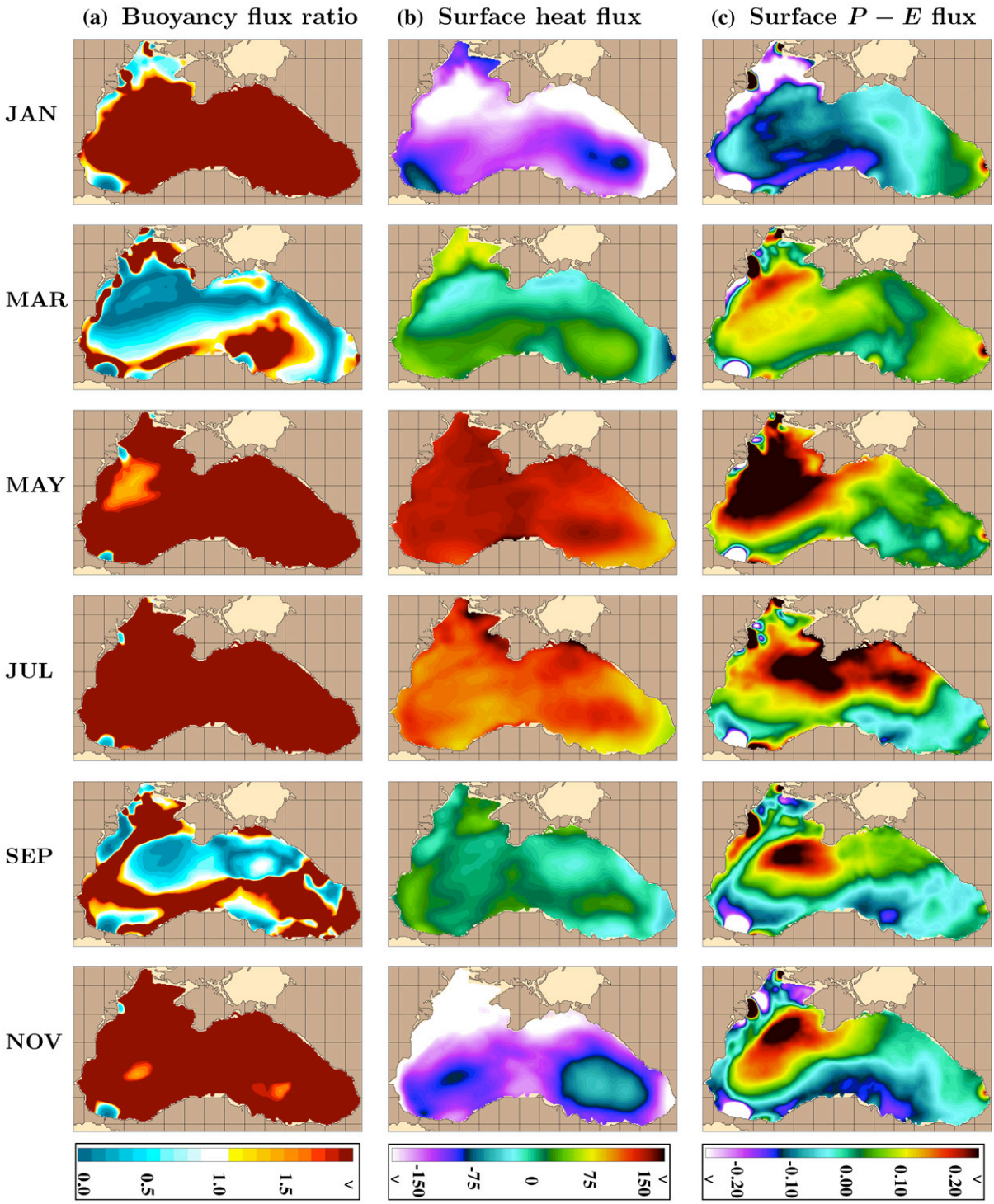

Fig. 7. (a) Buoyancy flux ratio (i.e., the ratio of the thermal buoyancy flux to saline buoyancy flux), (b) net heat flux at the sea surface (Q_a, in W m^{-2}), and (c) net freshwater flux at the sea surface (P–E in kg m^{-2} s^{-1}). All fields are obtained from the ≈3.2 km resolution HYCOM. Both E and P are in m s^{-1}, and they are multiplied by the density of ocean water at the sea surface to obtain the flux form. The P–E flux values in the figure are scaled by 10^3. In the model, we adopted the convention that all heat flux terms are positive into the ocean.

Please cite this article as: Kara, A.B., et al., Air–sea fluxes and river discharges in the Black Sea with a focus on the Danube and Bosphorus, J. Mar. Syst. (2008), doi:10.1016/j.jmarsys.2007.11.010

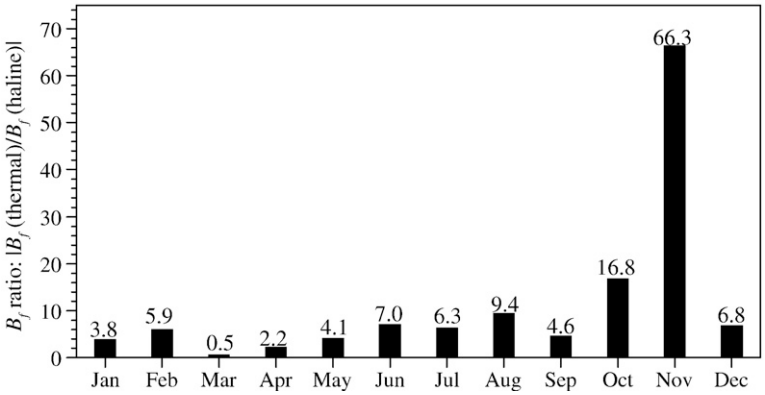

Fig. 8. The basin-averaged monthly mean buoyancy ratio values obtained from HYCOM in the Black Sea. Buoyancy ratio values are also written above histograms for each month. Note that the buoyancy ratio (i.e., the absolute value of the ratio of thermal buoyancy flux to saline buoyancy flux) is unitless.

generally positive (i.e., into the ocean) over the most of the Black Sea, and this is particularly seen in the western Black Sea from May to July (Fig. 7c). In these months, having $P–E>0$ implies $P>E$. Thus, relatively large precipitation values dominating over evaporation reduce turbulent mixing and produces the freshwater stratification. In a previous study, Cronin and McPhaden (1999), who examined the relationship between rainfall and salinity in the western equatorial Pacific, also found that rainfall generally produced a stable shallow layer when the net surface buoyancy flux stabilize the ocean surface layer, a result consistent with the shallow mixed layer formation in the Black Sea. In particular, the HYCOM simulation demonstrates that the largest and positive net freshwater flux values are seen from March through September in the Black Sea. Such a feature is consistent with estimations of net freshwater fluxes based on local data sets (Schrum et al., 2001). This result further confirms the existence of the shallow summer mixed layer due partly to the positive freshwater flux. However, the main reason for the shallow mixed layer is the net heat flux since the thermal buoyancy flux is much greater than haline buoyancy flux during summer (Fig. 8).

Finally, a possible formation of deep convection in the Black Sea is investigated by examining the monthly mean total buoyancy flux. As discussed in a theoretical and observational review study by Marshall and Schott (1999), who studied formation of convection over the various region of the global ocean, whether and when the deep convection occurs depends on the seasonal development of the surface buoyancy flux with respect to the initial stratification. In the case of the Black Sea, net heat flux is, for example, ≈ 100 W m^{-2} and $P–E$ is ≈ 1 m year^{-1} in the interior during summer. This implies a buoyancy flux of $\approx 10^{-8}$ m^2 s^{-3} over the interior. For stratification typical of the upper regions of the main thermocline, mixed layers do not reach great depth when exposed to buoyancy loss of these magnitudes, perhaps a several hundred meters or so. Since the stratification is very strong, and the total buoyancy flux is not sufficiently strong (e.g., $>10^{-7}$ m^2 s^{-3}) in the interior, convection is not expected to reach greater depths in the Black Sea on monthly time scales. In other words, the stratification inhibits convection.

The existence of relatively small surface thermal and haline surface fluxes is an indication of the fact that there is almost no deep convection in the Black Sea. However, the monthly climatological buoyancy fluxes may expected to be much weaker and smoothed than the episodic buoyancy forces operating over the ocean which drive the convection. The convection is an instantaneous process with a time scale of few days but HYCOM uses monthly climatological forcing (i.e., longer time scale). Thus, there are clearly differences in time scales between the model forcing and the convection episodes. On the other hand, we should state that the model forcing already includes 6 hourly high frequency component. Further research regarding possible existence of convection formation on shorter time scales (e.g., daily) deserves a future detailed study.

6. Model validation

This section presents evaluation of model results and, in particular examines whether or not the model is able to reproduce net heat flux at the sea surface, which was used for analyzing the buoyancy flux variations in the Black Sea. Although both HYCOM and ECMWF have zero basin-averaged annual mean heat net heat flux in the

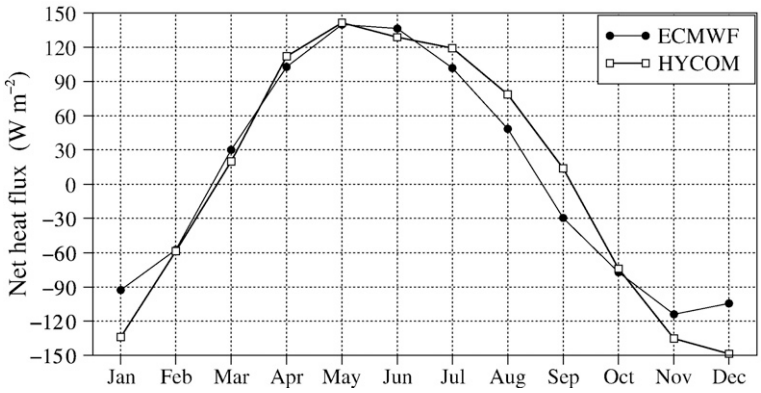

Fig. 9. The basin-averaged monthly mean climatological net flux at the sea surface from ECMWF over 1979–1993 and climatologically-forced 3.2 km resolution HYCOM simulation.

Black Sea, there are differences especially in summer, December and January (Fig. 9). The basin-averaged RMS net flux difference between HYCOM and ECMWF is 24 W m^{-2} over the seasonal cycle. This difference exists because HYCOM calculates latent and sensible heat fluxes based on the model SST (rather than ECMWF SST) at each time step, resulting in changes in the net heat flux. Such differences may also be caused by the land–sea mask used in ECMWF (Kara et al., 2007). For example, atmospheric forcing fields from ECMWF, as used in the HYCOM simulation, are contaminated by land values near the coast, thereby may result in unrealistic SSTs.

The zero net heat flux in HYCOM is maintained using the bulk parameterizations for latent and sensible heat fluxes. Essentially, there is a feedback between SST and net fluxes. Basing fluxes on the model SST automatically provides a physically realistic tendency towards the correct SST. In particular, any climatologically-forced (i.e., repeated year) simulation will have zero annual net heat flux, with the annual mean SST automatically adjusting to make this happen. Therefore any annual mean error will be in SST, rather than in the heat flux balance. This is clearly evident from Fig. 10, showing the basin-averaged monthly mean SSTs from HYCOM and a SST climatology as well. The monthly mean-based averaged climatology used for validating the model SST is based on the NOAA/NASA Pathfinder Advanced Very High Resolution Radiometer (AVHRR) data constructed over 1985–1997 (Casey and Cornillon, 1999). This data set represents a historical

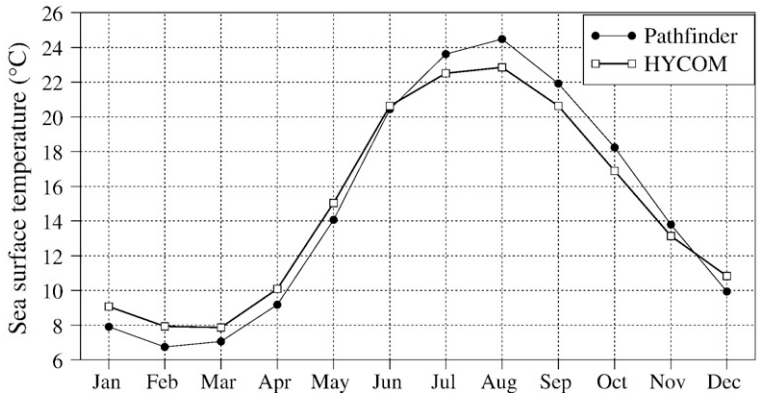

Fig. 10. The basin-averaged climatological monthly mean SST from the Pathfinder SST climatology and the 3.2 km resolution climatologically-forced HYCOM simulation. The monthly mean Pathfinder climatological SST used in this paper is based directly on satellite data during 1985–1997. It has a resolution of ≈9 km. This climatology is based directly on satellite data so it is treated as the "truth" in model-data comparisons. The Pathfinder SST climatology was interpolated to the Black Sea HYCOM domain before the basin-averaged monthly mean SSTs were calculated.

Please cite this article as: Kara, A.B., et al., Air–sea fluxes and river discharges in the Black Sea with a focus on the Danube and Bosphorus, J. Mar. Syst. (2008), doi:10.1016/j.jmarsys.2007.11.010

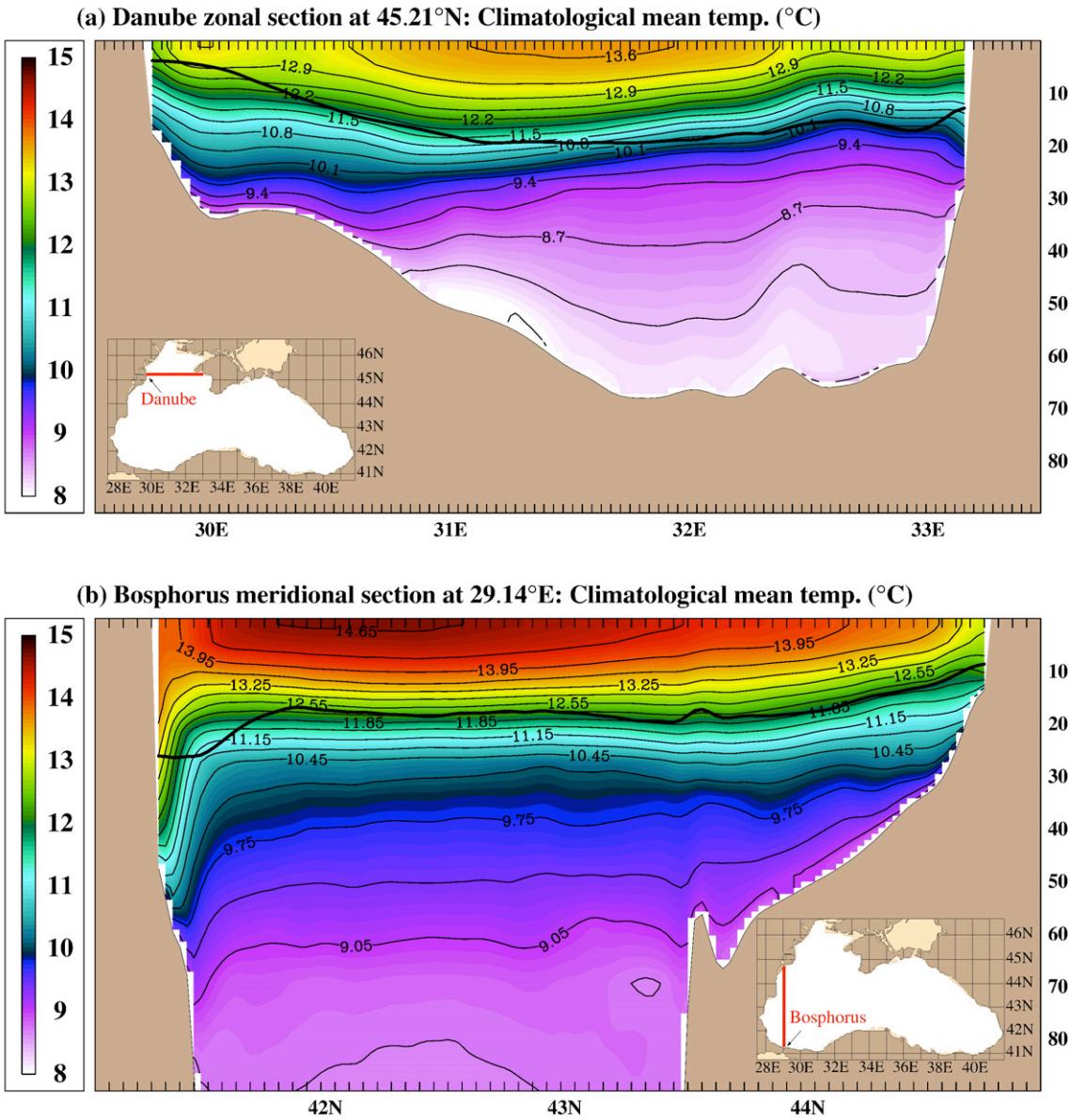

Fig. 11. Cross-sections of climatological annual mean temperature from the eddy-resolving ≈3.2 km resolution HYCOM simulation: (a) Simulated zonal sections in front of the Danube Delta at 45.21°N, and (b) meridional section through the Bosphorus Strait at 29.14°E. The thick solid line in black shows mixed layer depth diagnosed by the model whose calculation is explained in Kara et al. (2005d), in detail. The lines inside small sub-panels of the both figures illustrates the locations of Danube and Bosphorus sections.

reprocessing of the entire AVHRR time series using consistent SST algorithms, improved satellite and inter-satellite calibration, quality control and cloud detection.

Statistical metrics as used in Section 3 are also used for assessing the accuracy of monthly mean HYCOM SSTs in comparison to Pathfinder SSTs. The model gives an annual mean bias of −0.16 °C, and RMS SST difference of 0.98 °C over the seasonal cycle. Almost ≈97% of the observed Pathfinder SST variance can be explained by the HYCOM predictions since the basin-averaged correlation between the two is 0.98.

To further check on the model bias, a linear regression analysis is performed. If it is assumed that the HYCOM SST would fit the Pathfinder SST exactly, then a fit of the observed values to the model should show a linear slope with a zero intercept. However, a fit of the observed data using a linear fit to the model data gives a relationship, Pathfinder SST = −2.35 + 1.159 × (HYCOM SST) + error.

Please cite this article as: Kara, A.B., et al., Air–sea fluxes and river discharges in the Black Sea with a focus on the Danube and Bosphorus, J. Mar. Syst. (2008), doi:10.1016/j.jmarsys.2007.11.010

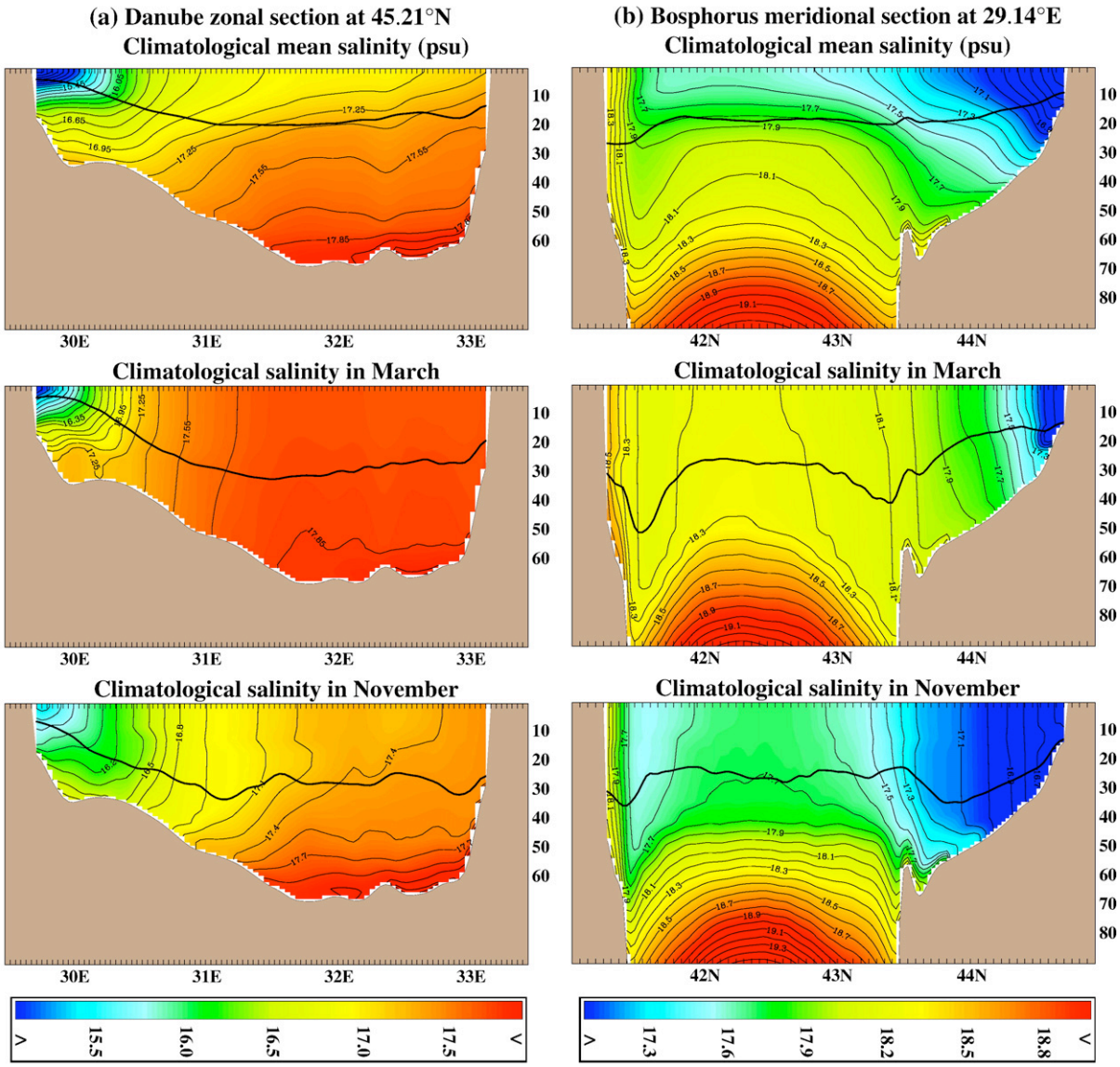

Fig. 12. The same as Fig. 11 but for cross-sections of climatological annual mean salinity along with and climatological mean salinities in March and November.

The linear equation can be recasted to show the nature of the bias as follows. Pathfinder SST = 14.78 + 1.159 × (HYCOM SST − 14.78) + error, where the annual mean model SST is 14.78 °C. The error has an estimated standard deviation of 0.69 °C. These results demonstrate that HYCOM is biased, with the bias changing at about 14.78 °C, and the bias increases away from 14.8 °C, larger for larger values and smaller for smaller values of the model prediction. If HYCOM has only random sources of error in prediction, we expect the slope to be 1.The null hypothesis is tested that the slope in the model is one against the alternate hypothesis that the slope is not 1.We found a t value of 0.159/0.036 = 4.4 with a two sided p value of 0.0016. Thus, the null hypothesis is rejected, and it is accepted that HYCOM has non-random sources of error.

HYCOM is also validated using subsurface temperature and salinity fields. Major features of the thermohaline fields in the Black Sea are the diluted surface water (salinity, which is about two times smaller than in the Mediterranean Sea) and the CIL, a layer where the temperature shows a persistent minimum of < 8°C. The latter generally extends to depths 50–100 m, where the downward propagation of the thermal signals from sea

Please cite this article as: Kara, A.B., et al., Air–sea fluxes and river discharges in the Black Sea with a focus on the Danube and Bosphorus, J. Mar. Syst. (2008), doi:10.1016/j.jmarsys.2007.11.010

surface is blocked by the extremely stable stratification. This vertical stratification varies locally as a consequence of dynamics and specific distribution of sources.

HYCOM presented in this paper realistically simulates most of the above mentioned features. For example, Fig. 11 shows vertical cross-sections of climatological annual mean of subsurface temperatures through two important regions where the model Black Sea is diluted (the area of Danube River plume) or receives salt (the area of the Bosphorus Strait). These fields are calculated by averaging the individual daily model output during 4 years of integration. The warm surface layer seen in the annual mean temperature extends to only about 20–40 m. Below this depth the cold water persists throughout the year. The local minimum gives an indication about CIW having its source on the continental slope. This cold plume is trapped by the slopped bottom and propagates southwards along the western coast, clearly revealing the HYCOM success in simulating coastal processes.

The annual mean salinity pattern illustrates the fact that the major dilution of the surface layers is caused by the river runoff (Fig. 12). The compensation of the excess of freshwater over most of the Black sea surface is prescribed in the model in a narrow vicinity of the Bosphorus Strait. The strongly concentrated source of positive buoyancy penetrates into the deeper layers as a vertical buoyant plume. The plume is vertical down to about 50 m, which is approximately the depth of the shelf north of the Bosphorus Strait. Below this depth the current behaves as a gravity flow reaching depths more than 100 m before losing its identity (Fig. 12b), which is also mentioned by Korotaev et al. (2001). The transport by the buoyant plume provides a continuous source of salty water helping to maintain the stratification of the Black Sea. The phenomenology of the simulated outflow justifies the approach chosen in this paper to introduce the strait outflow as a negative precipitation at the sea surface.

The sensitivity of salinity in the upper layer to the temporal variability in the freshwater is also revealed by an examination of subsurface salinity fields (Fig. 12a,b). The major differences are observed close to the source areas (the Danube Delta and the Bosphorus Strait). Here, one important result has to be made clear. Although the chosen periods (March and November) correspond to periods of relatively higher (lower) precipitation (runoff), the salinity in the surface layer is larger in March. This is explained by the larger mixing in the winter period and can be seen in the more diffusive halocline in March. On the opposite, the seasonal thermocline reduces mixing in the upper layer making the signature of freshwater more clear in fall. The volume occupied by the fresh coastal current is highly variable throughout the year demonstrating that this buoyancy signal shapes to a large extent the dynamics of the Western Black Sea.

7. Summary and conclusions

An examination of freshwater fluxes along with net heat fluxes at the sea surface through the buoyancy flux is essential in the Black Sea because they influence simulation of upper ocean quantities. Similarly, an accurate modeling of buoyancy fluxes is of particular importance in the region due to relatively large salinity gradients in the vicinity of riverine or estuarine discharge. Given that the river runoff has large influence on the dynamics of the continental shelf by changing the heat and freshwater fluxes, especially in the northwestern shelf, a database of accurate river flow estimates is useful to support various types of studies, including observational and modeling efforts in the Black Sea. For example, use of the reliable river database also enables an OGCM to more realistically represent variability and distribution of near-shore salinity in the vicinity of large rivers. It also provides a centralized source for estimates of river discharge of all rivers, even smaller rivers which might be insignificant in a coarse resolution OGCM but might be significant in a high-resolution OGCM. In this paper, a specific attention is therefore given to rivers discharged into the Black Sea.

River runoff values discharged into the Black Sea are obtained and compared to each other from four climatological data sources. Based on the statistical analysis, monthly mean river discharge values from all data sets are usually close to each other, and this is true for all six major rivers (Danube, Dniepr, Dniestr, Rioni, Sakarya and Kizilirmak). Although the monthly mean river discharge values for Danube and Dniestr show some differences when comparing RivDIS, UCAR and NRL climatologies, these differences are negligible. In the case of the Danube River, which has the largest discharge in comparison to other rivers, the monthly mean discharge values from RivDIS are only 1.8% (2.1%) different from the UCAR (NRL) climatologies. Similarly, the discharge values from UCAR are ≈1.3% different from RivDIS, indicating a remarkable agreement between the two data sets even though UCAR reports discharge values far away from the river mouth. Using these river discharge value we also analyze freshwater flux balance in the Black Sea. Overall, the rivers provide $\approx 287\ km^3\ year^{-1}$, precipitation accounts for $\approx 220\ km^3\ year^{-1}$, evaporation removes $\approx 270\ km^3\ year^{-1}$, and outflow through the Bosphorus is $\approx 217\ km^3\ year^{-1}$.

Following the analysis of the river data sources and freshwater flux balance, a climatologically-forced Black

Please cite this article as: Kara, A.B., et al., Air–sea fluxes and river discharges in the Black Sea with a focus on the Danube and Bosphorus, J. Mar. Syst. (2008), doi:10.1016/j.jmarsys.2007.11.010

Sea simulation was performed to calculate net buoyancy flux along with its components, i.e., buoyancy due to net heat flux (thermal buoyancy flux) and buoyancy due to freshwater flux at the sea surface (haline buoyancy flux). The fine resolution (≈3.2 km) HYCOM simulation is aimed to discuss the relative contributions of heat and salt fluxes at the ocean surface to the surface buoyancy flux in the Black Sea. A buoyancy gain (i.e., the upper ocean stabilizes) is evident in the Black Sea from March through September. On the contrary, a buoyancy loss (i.e., the upper ocean destabilizes) in other months. The thermal buoyancy flux is much greater than the haline buoyancy flux in all months except for March when the freshwater flux dominates the net heat flux. Thus, it is concluded that the seasonal variations of the heat flux is the major contributor to the buoyancy flux in the Black Sea. October is found to be the only time when thermal and haline buoyancy fluxes have different signs. In particular, thermal buoyancy flux destabilizes the upper ocean, while haline buoyancy flux stabilizes the upper ocean in October. Because the thermal buoyancy flux is much larger than the haline buoyancy flux, turbulence mixing is expected during the predawn rainfall. While the thermal flux is seasonally more dominant, local effects of haline contribution can be very important at some regions. We also speculate that since the magnitude of total buoyancy flux is not sufficiently strong in the Black Sea, convection should not be expected to reach greater depths in the Black Sea.

HYCOM is able to predict net surface heat fluxes with a RMS difference of 24 W m^{-2} in comparison to those from ECMWF over the seasonal cycle. HYCOM also maintains net zero net heat flux at the sea surface by using bulk parameterizations to calculate latent and sensible heat fluxes based on the model SST at each time step. Comparisons of basin-averaged monthly mean HYCOM SSTs with those from a satellite-based Pathfinder data set demonstrates that the model gives an annual mean SST bias of −0.16 °C, and RMS SST difference of 0.98 °C over the seasonal cycle. Thus, the Black Sea HYCOM is able to predict both net heat fluxes and SST with reasonable accuracies.

The use of river forcing as an addition to the precipitation field in ocean models is fairly often used, although sometimes it is handled as a spread-out land-runoff evenly distributed at the coastline rather than rivers. There is not much justification for it locally (i.e., for representing where river water advects to), but in principle, our experience demonstrates that it improves the basin-wide salt balance. In addition, while the non-existence of typical deep convection is revealed in this paper on climatological time scales, a detailed study is needed to further examine possible formation of such events on various time scales.

Acknowledgments

The HYCOM simulation was performed under the Department of Defense High Performance Computing Modernization Program on an IBM SP POWER3 at the Naval Oceanographic Office, Stennis Space Center, Mississippi. This work is a contribution of the 6.2 HYbrid Coordinate Ocean Model and advanced data assimilation, the NOPP HYCOM consortium for data-assimilative ocean modeling, and the 6.1 Thermodynamic and Topographic Forcing of Global Ocean Models projects. Funding was provided by the Office of Naval Research (ONR) under program elements 602435N for 6.2 and 601153N for 6.1 projects. E. Stanev's visit to NRL was supported by ONR office of London, U.K. We would like to thank C. N. Barron and L. F. Smedstad, both at the Oceanography Division of the Naval Research Laboratory (NRL), for discussion regarding the NRL river climatology data set. Reviewers provided excellent comments, and we would like to thank them for their criticisms. Very special thanks go to T. Oguz for various discussions about the Black Sea climate studies. This paper is contribution NRL/JA/7304/05/6067 and has been approved for public release.

References

Altman, E.N., Kumish, N.I., 1986. Interannual and seasonal variability of the Black Sea fresh water balance. Tr. Gos. Okeanogr. Inst. 145, 3–15 (in Russian).

Barron, C.N., Smedstad, L.F., 2002. Global river inflow within the Navy Coastal Ocean Model. Proc. Oceans 2002 MTS/IEEE Conf., 29–31 October, pp. 1472–1479.

Bleck, R., 2002. An oceanic general circulation model framed in hybrid isopycnic-Cartesian coordinates. Ocean Model. 4, 55–88.

Brydon, D., Sun, S., Bleck, R., 1999. A new approximation of the equation of state for seawater, suitable for numerical ocean models. J. Geophys. Res. 104. doi:10.1029/1998JC900059:1537–1540.

Casey, K.S., Cornillon, P., 1999. A comparison of satellite and in situ based sea surface temperature climatologies. J. Climate 12, 1848–1863.

Chassignet, E.P., Smith, L.T., Halliwell Jr, G.R., Bleck, R., 2003. North Atlantic simulations with the HYbrid Coordinate Ocean Model (HYCOM): impact of the vertical coordinate choice, reference pressure, and thermobaricity. J. Phys. Oceanogr. 33, 2504–2526.

Cronin, M.F., McPhaden, M.J., 1999. Diurnal cycle of rainfall and surface salinity in the western Pacific warm pool. Geophys. Res. Lett. 26, 3465–3468.

Czaya, E., 1981. Strome der Erde. Aulis-Verlag Deubner, Koln, Germany. 247 pp.

Degens, E.T., Kempe, S., Richey, J.E., 1991. Summary: biogeochemistry of major world rivers. In: Degens, E.T., Kempe, S., Richey, J.E. (Eds.), Biogeochemistry of Major World Rivers. John Wiley & Sons, New York, pp. 323–347.

Dai, A., Trenberth, K.E., 2002. Estimates of freshwater discharge from continents: latitudinal and seasonal variations. J. Hydrometeorol. 3, 660–687.

Dingman, S.L., 1994. Physical Hydrology. Prentice Hall, New Jersey. 575 pp.

Doney, S.C., Large, W.G., Bryan, F.O., 1998. Surface ocean fluxes and water-mass transformation rates in the coupled NCAR Climate System Model. J. Climate 11, 1420–1441.

Dynesius, M., Nilsson, C., 1994. Fragmentation and flow regulation of river systems in the northern third of the world. Science 266, 753–762.

Gibson, J.K., Kallberg, P., Uppala, S., Hernandez, A., Nomura, A., Serrano, E., 1999. ECMWF Re-Analysis Project Report Series: 1. ERA description (Version 2). 74 pp. [Available from ECMWF, Shinfield Park, Reading, RG2 9AX, UK.].

Halliwell Jr., G.R., 2004. Evaluation of vertical coordinate and vertical mixing algorithms in the HYbrid Coordinate Ocean Model (HYCOM). Ocean Model. 7, 285–322.

Kammerer, J.C., 1989. Large rivers of the world. American Geological Institute Data Sheet 85.1. Washington, D.C, U.S. Geological Survey.

Kara, A.B., Hurlburt, H.E., Wallcraft, A.J., Bourassa, M.A., 2005a. Black Sea mixed layer sensitivity to various wind and thermal forcing products on climatological time scales. J. Climate 18, 5266–5293.

Kara, A.B., Wallcraft, A.J., Hurlburt, H.E., 2005b. A new solar radiation penetration scheme for use in ocean mixed layer studies: an application to the Black Sea using a fine resolution HYbrid Coordinate Ocean Model (HYCOM). J. Phys. Oceanogr. 35, 13–32.

Kara, A.B., Wallcraft, A.J., Hurlburt, H.E., 2005c. Sea surface temperature sensitivity to water turbidity from simulations of the turbid Black Sea using HYCOM. J. Phys. Oceanogr. 35, 33–54.

Kara, A.B., Wallcraft, A.J., Hurlburt, H.E., 2005d. How does solar attenuation depth affect the ocean mixed layer? Water turbidity and atmospheric forcing impacts on the simulation of seasonal mixed layer variability in the turbid Black Sea. J. Climate 18, 389–409.

Kara, A.B., Hurlburt, H.E., Wallcraft, A.J., 2005e. Stability-dependent exchange coefficients for air–sea fluxes. J. Atmos. Ocean. Technol. 22, 1077–1091.

Kara, A.B., Wallcraft, A.J., Hurlburt, H.E., 2007. A correction for land contamination of atmospheric variables near land–sea boundaries. J. Phys. Oceanogr. 37, 803–818.

Kempe, S., Pettine, M., Cauwet, G., 1991. Biogeochemistry of European rivers. In: Degens, E.T., Kempe, S., Richey, J.E. (Eds.), Biogeochemistry of Major World Rivers. John Wiley & Sons, pp. 169–211.

Korotaev, G.K., Saenko, O.A., Koblinsky, C.J., 2001. Satellite altimetry observations of the Black Sea level. J. Geophys. Res. 106, 917–933.

Korotaev, G.K., Oguz, T., Riser, S., 2006. Intermediate and deep currents of the Black Sea obtained from autonomous profiling floats. Deep-Sea Res. 11 (53), 1901–1910.

Large, W.G., Danabasoglu, G., Doney, S.C., MeWilliams, J.C., 1997. Sensitivity to surface forcing and boundary layer mixing in a global ocean model: annual-mean climatology. J. Phys. Oceanogr. 27, 2418–2447.

Leopold, L.B., 1962. Rivers. Am. Sci. 50, 511–537.

Marshall, J., Schott, F., 1999. Open-ocean convection: observations, theory, and models. Rev. Geophys. 37, 1–64.

Meybeck, M., 1988. How to establish and use world budgets of riverine materials. In: Lerman, A., Meybeck, M. (Eds.), Physical and Chemical Weathering in Geochemical Cycles. Kluwer, Norwell, Mass., pp. 247–272.

Miller, J.R., Russell, G.L., Caliri, G., 1994. Continental-scale river flow in climate models. J. Climate 7, 914–928.

Milliman, J.D., Meade, R.H., 1983. Worldwide delivery of river sediments to the oceans. J. Geol. 91, 1–21.

Murphy, A.H., 1988. Skill scores based on the mean square error and their relationships to the correlation coefficient. Mon. Weather Rev. 116, 2417–2424.

Neter, J., Wasserman, W., Whitmore, G.A., 1988. Applied Statistics. Allyn and Bacon, Boston. 1006 pp.

Oguz, T., Ozsoy, E., Latif, M.A., Sur, H.I., Unluata, U., 1990. Modeling of hydraulically controlled exchange flow in the Bosphorus Strait. J. Phys. Oceanogr. 20, 945–965.

Oguz, T., Malanotte-Rizzoli, P., Aubrey, D., 1995. Wind and thermohaline circulation of the Black Sea driven by yearly mean climatological forcing. J. Geophys. Res. 100, 6845–6863.

Oguz, T., Besiktepe, S., 1999. Observations on the Rim Current structure, CIW formation and transport in the western Black Sea. Deep-Sea Res., Part 1 46, 1733–1753.

Ozsoy, E., Iorio, D.D., Gregg, M.C., Backhaus, J.O., 2001. Mixing in the Bosphorus Strait and the Black Sea continental shelf: observations and a model of the dense water outflow. J. Mar. Syst. 31, 99–135.

Perry, G.D., Duffy, P.B., Miller, N.L., 1996. An extended data set of river discharges for validation of general circulation models. J. Geophys. Res. 101, 21,339–21,349.

Schrum, C., Staneva, J., Stanev, E., Ozsoy, E., 2001. Air-sea exchange in the Black Sea estimated from atmospheric analysis for the period 1979–1993. J. Mar. Syst. 31, 3–19.

Showers, V., 1979. World Facts and Figures. John Wiley, New York. 757 pp.

Stanev, E.V., Bowman, M.J., Peneva, E.L., Staneva, J.V., 2003. Control of Black Sea intermediate water mass formation by dynamics and topography: comparison of numerical simulations, survey and satellite data. J. Mar. Res. 61, 59–99.

Staneva, J.V., Stanev, E.V., 1998. Oceanic response to atmospheric forcing derived from different climatic data sets. Ocean. Acta 21, 393–417.

Szestay, K., 1982. River basin development and water management. Water Qual. Bull. 7, 155–162.

Trenberth, K.E., Caron, J.M., Stepaniak, D.P., 2001. The atmospheric energy budget and implications for surface fluxes and ocean heat transports. Clim. Dyn. 17, 259–276.

United Nations Educational Scientific and Cultural Organization (UNESCO), 1985. Discharge of Selected Rivers of the World, vol. I, 11, I11 (Parts I, 11, 111, IV). UNESCO, Paris, France.

Unluata, U., Oguz, T., Latif, M.A., and Ozsoy, O., 1990. On the physical oceanography of the Turkish straits. In: Pratt, L.J. (Ed.), The Physical Oceanography of the Sea Straits, NATO/ASI Series, 318, Kluwer, Dordrecht, 25–60.

Vorosmarty, C.J., Sharma, K., Fekete, B.M., Copeland, A.H., Holden, J., Marble, J., Lough, J.A., 1997. The storage and aging of continental runoff in large reservoir systems of the world. Ambio 26, 210–219.

Vorosmarty, C.J., Fekete, B.M., Tucker, B.A., 1998. Global River Discharge Database (RivDIS) V1.1. [Available online at http://www.daac.ornl.gov.].

van der Leeden, F., 1975. Water Resources of the World. Water Information Center, Port Washington, New York. 568 pp.

van der Leeden, F., Troise, F.L., Todd, D.K., 1990. The Water Encyclopedia. Lewis Publishers, Chelsea, MI. 808 pp.

Webster, P.J., 1994. The role of hydrological processes in ocean–atmosphere interactions. Rev. Geophys. 32, 427–476.

Wijffels, S.E., 2001. Ocean transport of fresh water. In: Siedler, G., Church, J., Gould, H. (Eds.), Ocean Circulation and Climate: Observing and Modelling the Global Ocean. Int. Geophys. Ser., vol. 77, pp. 475–488.

Wijffels, S.E., Schmitt, R.W., Bryden, H.L., Stigebrandt, A., 1992. Transport of freshwater by the oceans. J. Phys. Oceanogr. 22, 155–162.

Please cite this article as: Kara, A.B., et al., Air–sea fluxes and river discharges in the Black Sea with a focus on the Danube and Bosphorus, J. Mar. Syst. (2008), doi:10.1016/j.jmarsys.2007.11.010